

# MR Myocardial Perfusion Imaging: Insights on Techniques, Analysis, Interpretation, and Findings<sup>1</sup>

Monda L. Shehata, MD  
Tamer A. Basha, PhD  
Mohammad R. Hayeri, MD  
Dagmar Hartung, MD  
Oleg M. Teytelboym, MD  
Jens Vogel-Claussen, MD

**Abbreviations:** AIF = arterial input function, BIR = B<sub>1</sub>-independent rotation, CAD = coronary artery disease, CFR = coronary flow reserve, CNR = contrast-to-noise ratio, DE = delayed enhancement, EPI = echo-planar imaging, GRE = gradient-echo, HCM = hypertrophic cardiomyopathy, IR = inversion recovery, LAD = left anterior descending, LV = left ventricle, MPR = myocardial perfusion reserve, ROI = region of interest, SENSE = sensitivity encoding, SNR = signal-to-noise ratio, SR = saturation recovery, SSFP = steady-state free precession, TIC = time-intensity curve

**RadioGraphics** 2014; 34:1636–1657

**Published online** 10.1148/rg.346140074

**Content Codes:**  

<sup>1</sup>From the Department of Radiology, Mercy Catholic Medical Center, Darby, Pa (M.L.S., M.R.H., O.M.T.); Department of Medicine (Cardiovascular Division), Beth Israel Deaconess Medical Center and Harvard Medical School, Boston, Mass (T.A.B.); and Department of Radiology, Hannover Medical School, OE 8220, Carl-Neuberg-Str 1, 30625 Hannover, Germany (D.H., J.V.C.). Recipient of a Certificate of Merit award for an education exhibit at the 2013 RSNA Annual Meeting. Received March 9, 2014; revision requested June 13 and received July 15; accepted July 18. For this journal-based SA-CME activity, the authors, editor, and reviewers have no relevant relationships to disclose. **Address correspondence** to J.V.C. (e-mail: [vogel-claussen.jens@mh-hannover.de](mailto:vogel-claussen.jens@mh-hannover.de)).

## SA-CME LEARNING OBJECTIVES

After completing this journal-based SA-CME activity, participants will be able to:

- List the physiologic autoregulatory mechanisms of the myocardial circulation at rest and during stress.
- Describe the basic principles of cardiac MR perfusion imaging, including technique, data analysis, and pitfalls.
- Discuss the clinical applications of cardiac MR perfusion imaging and the effect on patient treatment and follow-up.

See [www.rsna.org/education/search/RG](http://www.rsna.org/education/search/RG).

## TEACHING POINTS

See last page

Coronary microcirculatory dysfunction has a fundamental role in the pathophysiology of ischemic coronary artery disease (CAD) as well as various other cardiovascular disorders. Invasive coronary angiography remains the standard of reference for diagnosis of CAD. Nevertheless, it has been well acknowledged that the degree of luminal narrowing of epicardial coronary lesions detected at angiography is a poor predictor of the functional severity of the lesion. Recent studies demonstrate that assessment of coronary microcirculatory function by means of noninvasive myocardial perfusion imaging helps increase diagnostic accuracy and guide medical decision-making. Among available diagnostic modalities, cardiac magnetic resonance (MR) perfusion imaging has evolved to become a reliable and robust tool providing accurate quantitative assessment of regional myocardial perfusion. Owing to its high spatial resolution, noninvasive nature, and absence of ionizing radiation, cardiac MR perfusion imaging has improved detection of clinically relevant CAD. It has also offered further insights into the understanding of various cardiovascular disorders resulting from coronary microvascular dysfunction in the absence of proximal flow-limiting CAD. Cardiac MR perfusion imaging is now routinely used in many centers and shows promise in evaluating patients with disorders beyond those of the epicardial coronary circulation. Recent implementation of high-field-strength magnets and rapid acquisition techniques have further contributed to expanding the role of cardiac MR perfusion imaging to include novel promising applications. In this article, we provide an overview of cardiac MR perfusion imaging, including techniques, image analysis, and clinical applications.

©RSNA, 2014 • [radiographics.rsna.org](http://radiographics.rsna.org)

## Introduction

Noninvasive assessment of myocardial perfusion can offer accurate diagnosis and risk stratification for patients with known or suspected coronary artery disease (CAD). This can be achieved through multiple sophisticated diagnostic imaging modalities, with single-photon-emission computed tomography (SPECT) as the most common clinically available technique. However, current imaging tools have limitations and drawbacks related to limited resolution and use of ionizing radiation.

Assessment and quantification of contrast material-enhanced first-pass myocardial perfusion using dynamic time-resolved cardiac magnetic resonance (MR) imaging has evolved to become a reliable diagnostic tool for assessment of CAD. In this article, we provide a synopsis of the basic principles of cardiac MR perfusion imaging, review its current state for assessment of the coronary circulation, and address its promising novel applications.

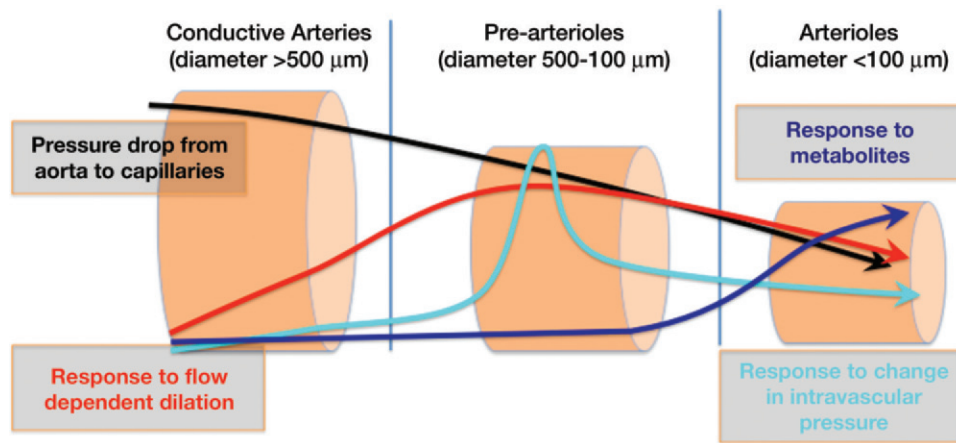


**Figure 1.** Functional anatomy and physiologic autoregulatory mechanisms of the coronary vascular bed. The coronary arterial system is composed of conductive arteries, prearterioles, and arterioles. The pressure drop is negligible in conductive arteries, appreciable in prearterioles, largest in arterioles. Conductive arteries and proximal prearterioles are responsive to flow-dependent dilatation. Distal prearterioles are more responsive than the other types of vessels to changes in intravascular pressure. Distal prearterioles and arterioles are the main sites of coronary blood flow autoregulation. (Adapted from reference 1.)

## Myocardial Circulation at Rest and Stress

The coronary circulation is a strictly regulated system that matches its blood flow with oxygen requirements through resistance coordination within its different domains, each governed by distinct regulatory mechanisms (1). These domains include (a) proximal epicardial coronary arteries (conductive arteries) (size range, 500 μm to 2–5 mm), which act mainly as capacitance vessels; (b) intermediate prearterioles (size range, 100–500 μm), which act to maintain pressure in response to perfusion pressure or flow change; and (c) intramural arterioles (size, <100 μm), which function mainly to match blood supply to the degree of oxygen consumption (Fig 1).

While the conductive arteries and proximal prearterioles are responsive to flow-dependent dilatation, distal prearterioles are more responsive to perfusion pressure changes. On the other hand, arterioles are highly responsive to metabolic regulation as a result of an increase in oxygen demand. This makes the distal prearterioles and arterioles the main site of coronary blood flow autoregulation.

Subsequently, in the setting of CAD, narrowing of the conductive arteries is expected to elicit vigorous neuronal and metabolic autoregulation processes at the level of the distal prearterioles and arterioles to maintain blood flow by lowering distal resistance. **While myocardial blood flow may remain normal for up to ~85% luminal diameter stenosis of the epicardial artery at rest, it is reduced during maximal hyperemia when the luminal diameter falls below 50% (2), thus unveil-**

**ing underlying autoregulatory decompensation at the level of the coronary microvascular bed.**

These findings have established the main principles of stress perfusion imaging based on the concept of coronary flow reserve (CFR):

$$CFR = CF_{\text{hyperemic}} / CF_{\text{resting}}$$

where  $CF$  = coronary flow. CFR reflects the magnitude of increase in coronary flow that can be achieved from the resting state to maximal vasodilatation. Since flow resistance is primarily determined by microvascular autoregulation, CFR is therefore considered a measurement of the function of the small vessels (3). This can be measured with phase-contrast MR imaging techniques by direct quantification of blood flow velocity in the lumen of the proximal and mid epicardial coronary arteries.

On the other hand, myocardial perfusion refers to the blood flow in the coronary bed passing from the epicardial vessels, through the arterioles, into the capillary bed where oxygen extraction takes place, and finally through the venous network. In principle, myocardial perfusion and oxygen supply through the microvascular bed is directly correlated with the myocardial blood flow.

In myocardial perfusion reserve (MPR) studies using perfusion agents such as gadolinium contrast material, the myocardial concentration of these agents is fundamentally related to the microvascular permeability–surface area product as well as the arterial concentration and flow. Hence, cardiac MR perfusion imaging entails characterization of the blood flow in the myocardium by measuring the amount of labeled substance that traverses a

unit volume of tissue per unit time. This in turn makes MPR measurement using SPECT or cardiac MR perfusion agents an indirect way of measuring CFR.

This relationship stands in the healthy coronary circulation. However, in the presence of flow-limiting epicardial disease, CFR can be lower in magnitude compared with the perfusion reserve in the presence of coronary collaterals. This renders MPR a more sensitive measurement of microvascular function in the setting of CAD. Hence, it is currently used as a surrogate marker for detection of ischemia.

MPR reflects myocardial blood flow through the coronary microcirculation (ie, blood volume flowing through a unit myocardial mass per unit time) during the maximal vasodilatation state versus during the resting state. These measurements are obtained through dynamic tracking of the myocardial signal change as a result of magnetization alteration induced by the first pass of a tight bolus of administered contrast agent, a concept described by Miller et al (4) and modified by Atkinson et al (5).

## Principles of MR Myocardial Perfusion Imaging

### Cardiac MR Perfusion Tracers

There are two major methods of arterial blood labeling for cardiac MR perfusion analysis: exogenous tracer labeling and endogenous tracer techniques.

**Exogenous Tracers (Contrast Agents).**—The first and more widely applicable method is achieved using exogenous tracer labeling by administration of gadolinium-based contrast agents and imaging during the first pass of contrast agent through the cardiac chambers, a method also referred to as first-pass perfusion imaging. Because gadolinium is a paramagnetic material, gadolinium-based contrast agents administered at a low dose alter the local magnetic field, thereby enhancing the relaxation rate of the myocardial water protons in proximity to the contrast agent. This in turn results in high T1 signal in the perfused myocardium. The conventional extravascular extracellular class of contrast agents is generally formed of small molecules that can easily diffuse from the intravascular to the extravascular compartment.

Intravascular gadolinium-based agents are the second class of exogenous agents, which are characterized by large molecular size, limiting free diffusion into the extravascular compartment. While these agents were initially developed for MR angiography, several groups have identified

their advantages for cardiac MR perfusion imaging, including more prolonged differentiation of ischemic from remote myocardium (6,7).

Demonstration of hypoperfusion secondary to flow-limiting epicardial lesions or microvascular dysfunction requires administration of contrast material as a tight bolus at a rapid injection rate of 4–5 mL/min through a wide-bore line. This helps eliminate injection rate as a limiting factor for myocardial enhancement during the first pass of contrast material.

**Endogenous Tracers.**—As in other parts of the body, using endogenous tracer techniques in cardiac MR perfusion imaging generally carries the advantage of eliminating contrast agent side effects. Hence, it could be safely performed in patients who are not candidates for first-pass cardiac MR perfusion imaging (eg, patients with end-stage renal disease).

Arterial spin labeling (ASL) MR imaging is a non-contrast agent technique that has been applied for quantification of tissue blood flow. In the ASL technique, blood is labeled as an endogenous tracer by applying a spatially selective inversion preparation, followed by tracking of the signal changes that result from flow of the inverted spins into or out of an adjacent region. While there are favorable published research data about ASL myocardial stress testing (8), its application in clinical settings remains limited because of the confounding effects of cardiac motion and the relatively modest signal changes achievable.

Blood oxygen level-dependent (BOLD) myocardial imaging is another promising alternative approach (9). As with ASL, BOLD imaging remains confined to experimental studies, facing challenges mainly related to limited contrast-to-noise ratio (CNR).

### Stress Testing

The objective of all forms of stress testing in CAD is to assess the extent and amount of the hyperemic response of the coronary circulation (ie, measurement of CFR or MPR during MR stress perfusion imaging). In general, stress tests can be categorized into pharmacologic and physiologic stress tests.

Exercise stress testing provides a physiologic direct link between exertional symptoms and coronary ischemia. To date, however, cardiac MR stress testing is almost exclusively performed with pharmacologic stress. Physical cardiac MR stress imaging, although applied in limited pilot studies (10), remains challenging due to the paucity of MR imaging-compatible exercise equipment as well as anticipated degraded image quality secondary to motion artifacts during physical activity.

**Table 1: Pharmacologic Stress Agents: Doses, Administration Routes, Mechanisms of Action, Contraindications, and Side Effects**

Stress Agent	Dose and Administration Route	Mechanisms of Action	Contraindications and Side Effects*
Dobutamine	Maximal dose 40 µg/kg/min; infusion	Direct B <sub>1</sub> and B <sub>2</sub> receptor stimulation with dose-related increase in heart rate, blood pressure, and myocardial contractility	Systemic hypertension Complex arrhythmia HOCM Uncontrolled CHF
Atropine	0.25-mg fractions typical (maximal dose 2 mg)	Nonselective muscarinic acetylcholinergic antagonist	Narrow-angle glaucoma Myasthenia gravis Obstructive uropathy
Adenosine	140 mg/kg/min dose; 4–6-min infusion	Activation of A <sub>1</sub> , A <sub>2B</sub> , and A <sub>3</sub> receptors Activation of the A <sub>2A</sub> receptors induces direct coronary arteriolar vasodilatation Half-life = 10 sec	Second- or third-degree AV block Systolic BP <90 mm Hg Active airway disease Hypersensitivity
Regadenoson	0.4-mg single injection	A <sub>2A</sub> receptor agonist inducing direct coronary vasodilatation Weak, if any, affinity for the A <sub>2B</sub> and A <sub>3</sub> adenosine receptors Initial phase half-life = 2–4 min followed by longer elimination phase of 2–4 h	Similar but reduced side effects in comparison with adenosine

Source.—Reference 11.

\*AV = atrioventricular, BP = blood pressure, CHF = congestive heart failure, HOCM = hypertrophic obstructive cardiomyopathy.

Hence, myocardial stress achieved with pharmacologic agents currently remains the most robust method to achieve adequate hyperemic response in the cardiac MR imaging environment. These agents may be further subdivided into primary coronary vasodilators (adenosine or regadenoson) and chronotropic inotropic agents (dobutamine). Detailed descriptions of the recommended dose, administration route, mechanism of action, and contraindications for each pharmacologic agent are given in Table 1.

Administration of vasodilator stress agents (eg, adenosine) in the MR imaging environment is a challenging process requiring special safety precautions. As proposed in the recent update on standardized cardiac MR imaging protocols (11), the imaging setting should be equipped with MR imaging-compatible monitoring devices like electrocardiographic and blood pressure monitors. Emergency resuscitation equipment should be readily available, including a defibrillator and an emergency cart equipped with emergency drugs and pharmacologic antidotes (ie, epinephrine, β-blockers, atropine, bronchodilators, as well as antiarrhythmic medications).

Adenosine and dobutamine have been the mainstays of cardiac MR vasodilator stress testing. In an attempt to limit the systemic side effects of adenosine, several selective A<sub>2A</sub> receptor

agonists have been examined as potential stress agents, out of which regadenoson (Lexiscan, Gilead Sciences, Foster City, Calif) was first to be approved recently by the U.S. Food and Drug Administration (12). Regadenoson offers several appealing features for clinical use, including relative ease of administration as a weight-unadjusted single bolus dose (0.4-mg single dose), fast onset and short duration of action, as well as efficacy comparable to that of adenosine (13) with fewer side effects. Hence, unlike adenosine, regadenoson could be used in patients with mild reactive airway disease and obstructive lung disease (12).

### Pulse Sequences and Imaging Protocols

**Pulse Sequences.**—Cardiac MR perfusion imaging has undergone steady improvement since it was proposed over 2 decades ago (5). Given the current advances in gradient technology, rapid acquisition and reconstruction techniques, as well as data analysis algorithms, a variety of pulse sequences are currently available for cardiac MR perfusion imaging. These include gradient-echo (GRE) (14), hybrid GRE-echo-planar imaging (EPI) (15), and steady-state free precession (SSFP) (16) sequences.

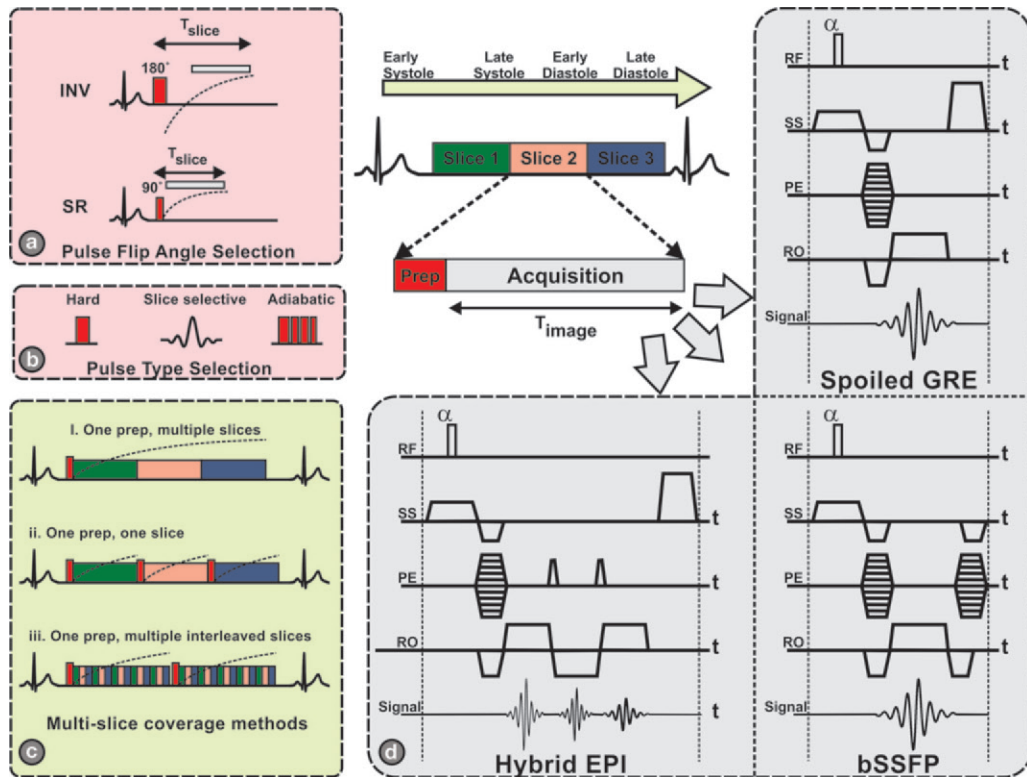


**Figure 2.** Perfusion imaging pulse sequence, timing diagrams, and pulse selection. On detection of the QRS complex, multiple sections are acquired after magnetization preparation.  $T$  = time. (a) Preparation pulses can be a  $180^\circ$  inversion (*INV*) pulse or a  $90^\circ$  saturation-recovery (*SR*) pulse. (b) The type of preparation pulse can be selected to be a very short nonselective hard pulse, a section-selective pulse, or an adiabatic pulse. (c) Multisection coverage can be achieved by using different approaches: a single preparation (*prep*) pulse for all sections, one preparation pulse for each section, or one preparation pulse for multiple interleaved sections to achieve the same CNR in all sections. (d) After preparation, image acquisition can be performed using different sequences: GRE, balanced SSFP (*bSSFP*), or a hybrid EPI sequence. *PE* = phase-encoding, *RF* = radiofrequency, *RO* = readout, *SS* = section-selective,  $t$  = time.

Selection of the appropriate pulse sequence is critical in determining the image contrast, spatial resolution, and coverage extent (Fig 2d). In addition, it also affects the analysis process by influencing the potential for quantification and/or the presence of artifacts. A description of available sequences and their advantages and disadvantages is presented in Table 2.

All perfusion imaging sequences entail dynamic imaging of the heart to allow a fraction-of-a-heartbeat acquisition that is repeated over a number of heartbeats to track the first pass and washout of the contrast agent bolus (Fig 3). This requires adequate temporal resolution, an adequate acquisition window, adequate spatial resolution, section coverage, strong T1 contrast in the commonly used T1-weighted sequence, and maintained signal linearity.

1. *Adequate temporal resolution* is critical for determining the time between two images at the same section location, hence affecting the ability to monitor changes in signal intensity and modeling of first-pass bolus kinetics. Typically,

images are acquired every one to two heartbeats for adequate sampling of the myocardial blood flow, whereas in the quantitative setting, accurate quantification of the arterial input function (AIF) may require left ventricular (LV) blood pool sampling every heartbeat.

2. *An adequate acquisition window* is primarily determined through the time per section ( $T_{\text{section}}$ ) within the cardiac cycle as well as the actual imaging readout time ( $T_{\text{imaging}}$ ), which in turn influences susceptibility to cardiac motion. (In general, the image acquisition time per section is  $\leq 200$  msec.)

3. *Adequate spatial resolution* helps achieve adequate transmural discrimination between subendocardial and subepicardial perfusion deficits. In a typical perfusion imaging acquisition, the in-plane resolution should preferably be kept to  $\leq 3$  mm. This is usually accomplished through a compromise between the spatial resolution, the number of sections covered, and the acquisition window.

For example, a typical field of view of  $320 \times 320$  mm<sup>2</sup> can be acquired by using an acquisition

**Table 2: Cardiac MR Perfusion Imaging Sequences: Descriptions, Acquisition Times, Advantages, and Disadvantages**

Sequences	Description	Average Acquisition Time	Advantages	Disadvantages
Turbo FLASH, turbo FFE, GRASS	GRE acquisition, short TR and TE Magnetization preparation	130–200 msec per section	Reduced motion and blood flow artifacts	Low SNR
Turbo SSFP, turbo balanced field echo, turbo FIESTA	SSFP acquisition Magnetization preparation	130–200 msec per section	Higher temporal resolution Higher SNR	Off-resonance artifacts Bolus-induced frequency shifts Not suitable for >1.5-T imaging
Hybrid EPI-GRE	Hybrid EPI-GRE acquisition with echo train length less than six Magnetization preparation	100–150 msec per section	Rapid acquisition	Susceptibility artifacts with long echo trains Echo train length <3 for 3-T imaging

Source.—Reference 3.

Note.—FFE = fast field echo, FIESTA = fast imaging employing steady-state acquisition, FLASH = fast low-angle shot, GRASS = gradient-recalled acquisition in the steady state, SNR = signal-to-noise ratio, TE = echo time, TR = repetition time.

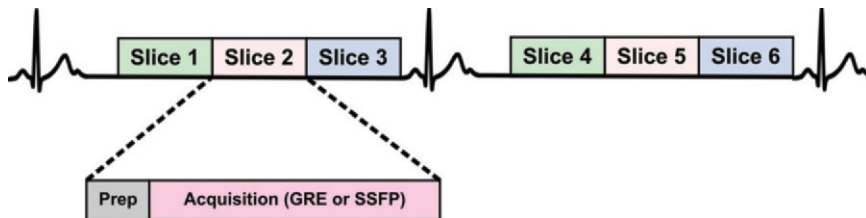


**Figure 3.** Typical first-pass perfusion imaging pulse sequence. Cardiac-gated acquisitions are performed by using an electrocardiographic signal. Multiple sections are acquired consecutively (eg, six sections every two R-R intervals, as shown). This is repeated continuously during the first pass and washout of the contrast agent. T1 contrast is generated by using a saturation preparation (*Prep*) pulse followed by fast acquisition of each section using a GRE, GRE-EPI, or SSFP sequence.

window of approximately 123 msec, achieving an in-plane spatial resolution of  $3 \times 3 \text{ mm}^2$  at an acquisition matrix size of  $107 \times 107$  and repetition time (TR) of 2.3 msec. However, to achieve a higher in-plane spatial resolution of  $2.5 \times 2.5 \text{ mm}^2$ , a longer acquisition window of approximately 154 msec, higher acquisition matrix size of  $128 \times 128$ , and longer TR of 2.4 msec are used, assuming that a standard parallel imaging acceleration factor of 2 is implemented in both cases. While the first imaging parameters provide a shorter acquisition window, which is less vulnerable to cardiac motion, the latter parameters offer better spatial resolution.

4. *Anatomic coverage:* It is always desirable to achieve greater myocardial coverage by increasing the number of acquired sections. However,

this is influenced by the patient's heart rate, which in turn determines the acquisition window. Imaging several sections during each cycle leads to variation in wall thickness and motion between sections, since each section is acquired at a different cardiac phase. On the other hand, limiting the acquisition to a specific phase of the cardiac cycle can result in less motion and myocardial thickness variation at the expense of less section coverage.

When the first technique is used, several approaches can be offered to optimize cardiac cycle utilization. In one approach, a shared SR pulse is applied followed by consecutive section acquisition. In another approach, several SR pulses are implemented, each followed by a single section acquisition. In both approaches, T1 contrast and

CNR will vary depending on the rate of signal recovery among the sections.

There are several options that can be used to either reduce these variations or increase the T1 contrast. By using an interleaved sections approach, the acquisition of two or more sections is interleaved after each SR pulse. This might increase the acquisition window but would generally result in uniform T1 contrast and CNR. A different approach involves application of notched SR pulses, where each SR pulse saturates the whole volume except a specific section, which is imaged after the next SR pulse (Fig 2c). This provides a longer inversion time, which in turn increases T1 contrast. In a typical perfusion imaging acquisition, three to six sections are usually acquired.

5. *Strong T1 contrast in the commonly used T1-weighted sequence* is needed to reflect the temporal change in contrast agent concentration, which is inversely related to myocardial T1. T1-weighted sequences are classified into two main categories based on the magnetization preparation pulse that is used: inversion recovery (IR) using a 180° inversion pulse and SR using a 90° saturation pulse (Fig 2a).

Previously, a 180° inversion pulse (17) was used for magnetization preparation (14). IR provides a larger dynamic signal range (recovering from  $-M_0$  to  $+M_0$ ) relative to SR—which has only half this range (recovering from  $-M_0$  to  $+M_0$ )—and thus results in stronger contrast. However, it requires more time for recovery, limiting multisection coverage per heartbeat, and the signal is usually dependent on the magnetization history, either from the previous section or the previous heartbeat, which makes it vulnerable to heart rate variations and different contrast between sections.

Currently, 90° SR providing better CNR has emerged as the more widely applied method to achieve T1 weighting (18). Despite its lower dynamic range, SR provides a higher contrast independent of magnetization history and heart rate variations. Moreover, it allows a higher number of sections to be acquired, increasing myocardial coverage. Typically, SR is implemented by using a nonselective 90° pulse followed by a crusher gradient. This has proved sensitive to  $B_1$  field variations. Thus, composite adiabatic radiofrequency pulses (eg,  $B_1$ -independent rotation-1 [BIR-1] and BIR-4) have been introduced to provide more uniform  $B_1$ -insensitive saturation effect (Fig 2b). However, this also comes with longer SR pulses, more radiofrequency heating deposition, and difficulty in employing any section-selective maneuvers like notched SR pulses.

6. *Maintained signal linearity*: A linear relationship between the administered contrast

agent concentration and the measured resulting signal is always desirable for proper perfusion quantification. This usually depends on two imaging parameters: the saturation or inversion delay (ie, the starting time of the acquisition relative to the saturation or inversion pulse) and the acquisition window.

A longer saturation delay allows imaging to occur at the flat part of the signal recovery curve and thus has a closer relation to the contrast agent concentration in the myocardium. However, this results in a CNR reduction, since the relative signal difference between low and high contrast agent concentration areas, which is the main factor for CNR, becomes smaller as the saturation delay becomes longer.

Reducing the acquisition window, usually in the range of 100–200 msec, also helps achieve a more linear relationship, since it reduces the variation range of the signal recovery curve between the starting and ending points of the acquisition. However, reducing the acquisition window is challenging and is usually accompanied by a spatial resolution loss or acceleration imaging artifacts if very high acceleration rates are used.

**Parallel Imaging.**—A pertinent initial obstacle to wide clinical application of cardiac MR perfusion imaging had been its limited temporal resolution, which led to decreased spatial coverage. This was more pronounced with a stress-induced increase in heart rate. Nowadays, implementation of parallel imaging techniques has helped circumvent these constraints (19). Also, the achieved imaging acceleration has allowed transition from multisection two-dimensional acquisitions to three-dimensional acquisitions covering the whole heart at 1.5-T imaging and recently extended to 3-T imaging, which appears promising (20).

Standard parallel imaging techniques (eg, sensitivity encoding [SENSE], generalized autocalibrating partially parallel acquisition [GRAPPA]) are currently commonly used in routine clinical perfusion acquisitions to reduce the acquisition window by a factor of two to four (21,22). Despite the associated SNR penalty, reducing the acquisition time allows either more coverage or higher spatial resolution.

Recently, spatiotemporal acceleration methods (eg, k-t SENSE, k-t BLAST [broad-use linear acquisition speed-up technique], k-t PCA [principal component analysis]) that exploit the redundancy of the data in the spatiotemporal dimension have been proposed to allow further reduction in the acquisition window, achieving acceleration factors as high as 12. Recent studies have also combined compressed sensing with

parallel imaging to exploit the sparsity in the k-t dimension, achieving acceleration factors of up to 24 (23).

However, such methods need special care, as they are very sensitive to motion and involve a lot of temporal smoothing, which might significantly affect perfusion quantification. The major challenge experienced with all new acceleration approaches is that reduction of the acquisition window generally affects different factors of the imaging process, and thus requires a lot of parameter optimization specific for each sequence and involves a lot of trade-offs for the output image features in terms of SNR, CNR, spatial resolution, and signal linearity, for example.

**1.5-T vs 3-T Imaging.**—3-T MR imaging units are becoming more widely available and are currently used on a larger scale for MR perfusion imaging. Although higher field strengths come with the advantage of higher SNR, there are several disadvantages that can result in artifacts affecting perfusion imaging and analysis. These include:

**Contrast agent dose:** The relaxivity of most of the commonly used gadolinium-based contrast agents decreases at higher field strengths, leading to less of a T1-shortening effect, which in turn results in reduction of CNR. However, this is usually not a major concern when the previously mentioned SR or IR techniques are used.

**B<sub>0</sub> and B<sub>1</sub> inhomogeneities:** Both B<sub>0</sub> and B<sub>1</sub> increase at 3 T, which requires more attention to B<sub>0</sub> and B<sub>1</sub> field inhomogeneities, especially with rapid acquisition imaging (eg, SSFP) or when special tailored radiofrequency pulses (eg, adiabatic BIR-4) are used.

**SNR, T2, and specific absorption rate (SAR):** At higher field strengths, myocardial T2 does not change much. However, with the increasing field inhomogeneity effect, the overall T2\* decreases, leading to signal reduction and thus lower SNR. This reduction can easily be compensated for by the large SNR gain achieved due to the higher field strength. However, this usually comes with a higher tissue energy deposition (ie, SAR), significantly limiting any possible high SNR gain. Such factors generally lead to a moderate increase in SNR at 3 T relative to that at 1.5 T (24,25).

**T1 and CNR:** T1 significantly increases at higher field strengths. In the presence of an adequate contrast agent dose, this results in a larger difference in T1 before and after contrast agent administration, leading to a better CNR.

**Imaging artifacts:** At higher field strength, the SNR increase introduces different types of artifacts that may influence perfusion imaging and analysis. For example, susceptibility artifacts are

known to be problematic at 3 T, especially when rapid imaging sequences (eg, SSFP) are used, requiring special shimming maneuvers including higher-order shimming utilization. This effect gets worse with perfusion imaging, where susceptibility artifacts are thought to be one of the contributing factors to dark rim artifacts.

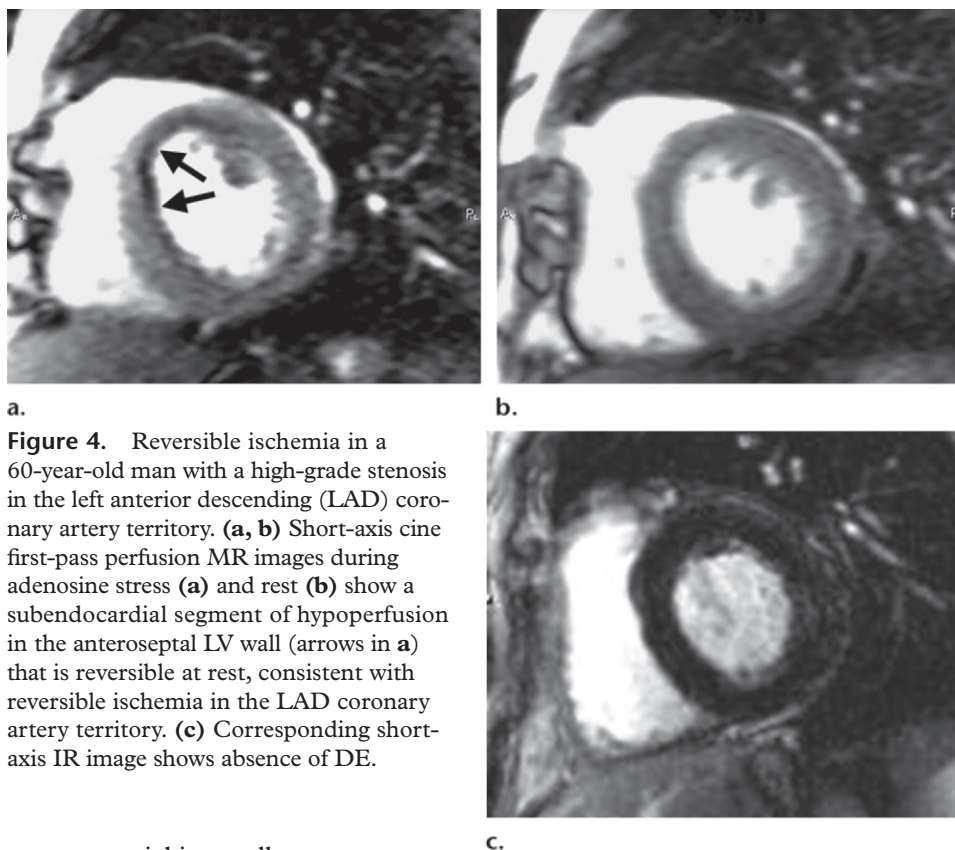
Overall, 3-T MR imaging looks promising for perfusion imaging, albeit with a few technical challenges. However, with 3-T imaging units gaining a bigger share of the MR imaging market, these technical problems are expected to be addressed in a way that will allow full exploitation of the capabilities of higher field strengths for perfusion imaging.

**Imaging Protocol.**—A detailed standardized cardiac MR perfusion imaging protocol was recently presented in the Society for Cardiovascular Magnetic Resonance task force 2013 update (11).

Three to six sections are routinely covered (typically three sections along the short axis with or without two- and four-chamber sections), with image acquisition at a temporal resolution of one to two R-R intervals at each section position. Different sections are acquired at different phases of the cardiac cycle, whereas each section is imaged at the same phase over multiple cycles. Systolic phase section acquisition generally results in increased myocardial thickness, hence limiting volume averaging during analysis, whereas diastolic phase section acquisition limits motion artifacts (18). A section thickness of 5–10 mm and in-plane resolution of 1.5–3 mm are typical parameters used for a multisection acquisition. Image acquisition per section can take on the order of 50–200 msec, depending on imaging parameters, image acceleration, and use of ultrafast imaging sequences (18).

Actual MR perfusion imaging parameters depend on imaging unit type, hardware, and heart rate. For example, the following MR imaging parameters may be applied when using a high-performance gradient system capable of 45 mT/m at a 200 mT/m/msec slew rate and an SR FLASH GRE sequence: echo time = 1.3 msec, repetition time = 2.2 msec, bandwidth = 780 Hz/pixel, echo train length = one, flip angle = 12°, matrix = 120 × 80, SENSE parallel imaging factor = 2, TD (trigger delay time to first line) = 41 msec, imaging time = 88 msec, total acquisition time per section = 130 msec, number of sections according to heart rate at 60, 90, and 120 beats per minute = seven, five, and three, respectively (14).

In a typical cardiac MR perfusion study, stress phase imaging typically precedes resting phase imaging by approximately 10 minutes to allow washout of gadolinium contrast material.



**a.**  
**Figure 4.** Reversible ischemia in a 60-year-old man with a high-grade stenosis in the left anterior descending (LAD) coronary artery territory. **(a, b)** Short-axis cine first-pass perfusion MR images during adenosine stress **(a)** and rest **(b)** show a subendocardial segment of hypoperfusion in the anteroseptal LV wall (arrows in **a**) that is reversible at rest, consistent with reversible ischemia in the LAD coronary artery territory. **(c)** Corresponding short-axis IR image shows absence of DE.

For visual analysis, contrast material is usually administered at a dose of 0.05–0.1 mmol/kg for both phases followed by an adequate saline flush (26). On the other hand, quantitative assessment of myocardial perfusion depends on a reliable determination of the AIF, which is the concentration of gadolinium contrast material in the LV or aortic blood pool as a function of time during its first pass and is usually measured in the LV or ascending aorta. This in turn requires arterial contrast enhancement sampling without too much saturation. The contrast enhancement should be in approximately linear relation to the concentration of contrast agent in the blood pool.

It has been demonstrated by Wendland et al (27) that T2\* saturation effects cause a nonlinear relationship between tracer concentration and MR signal at concentrations necessary to visualize differences in tracer uptake within the myocardium, subsequently affecting the true AIF, as later proved by Kellman et al (28). To address this question, “dual-bolus” (29,30) and “dual-sequence” (31–33) imaging strategies were proposed. In the dual-bolus strategy, AIF is measured from a low-dose bolus (1/10th or 1/20th of the dose) followed by a full dose at 0.05 mmol/kg. On the other hand, the dual-sequence strategy employs low-resolution dynamic imaging with short SR time for calculation of the AIF. This is followed by a high-resolution image for quantifying myocardial enhancement signal.

## Image Interpretation and Analysis

**Qualitative Interpretation.**—In the routine clinical setting, perfusion cine loops are reviewed and analyzed visually. Concomitant acquisition and interpretation of cardiac MR perfusion studies with delayed enhancement (DE) was shown to improve diagnostic accuracy in the setting of CAD (34). In their study, Klem et al (34) presented a stepwise analysis algorithm that starts with review of the DE images, followed by review of the stress phase images, and finally review of the resting phase images for identifying and classifying CAD.

Hypoperfused myocardium is generally identified as a hypointense area compared with remote (ie, normal) myocardium. A reversible stress-induced area of myocardial hypoperfusion usually lasting for eight heartbeats or longer in the absence of DE is consistent with underlying coronary ischemia (Fig 4). An area of irreversible myocardial hypoperfusion with matched DE is seen in the setting of myocardial infarction or scarring (Fig 5).

**Quantitative Analysis.**—Quantitative analysis of myocardial perfusion has been largely driven by the desire to obtain observer-independent and reproducible measures of myocardial perfusion

Teaching  
Point

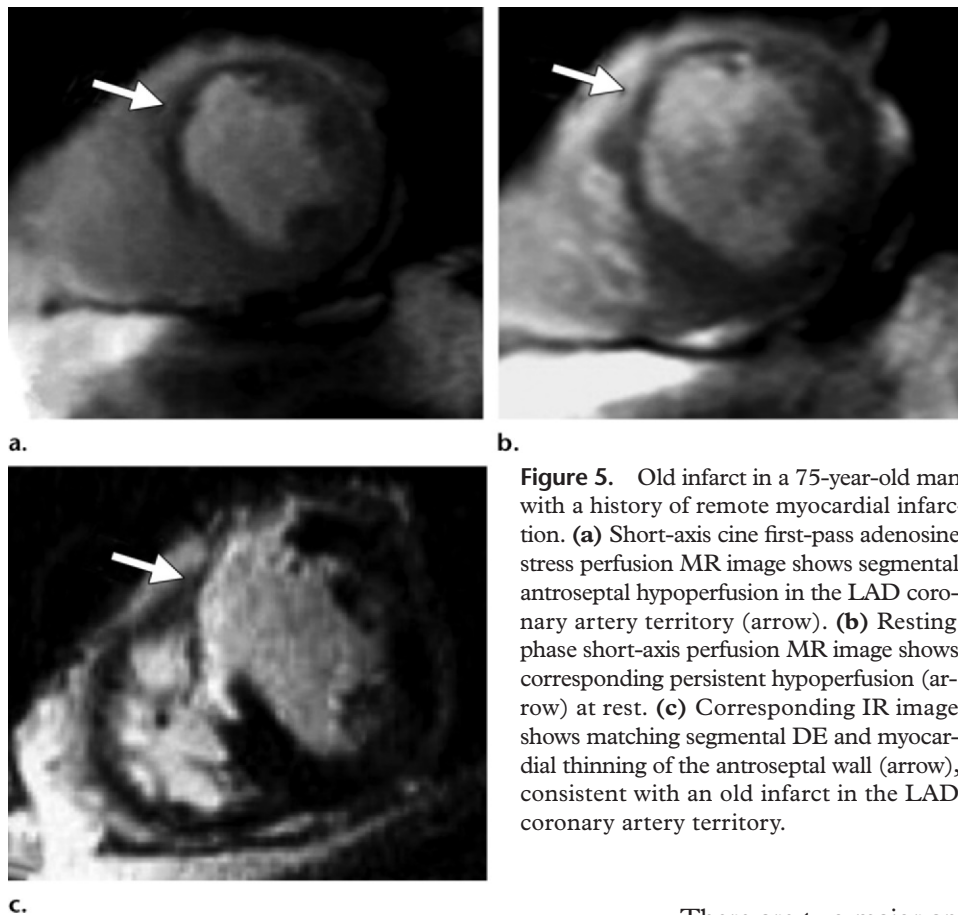


**Figure 5.** Old infarct in a 75-year-old man with a history of remote myocardial infarction. **(a)** Short-axis cine first-pass adenosine stress perfusion MR image shows segmental antroseptal hypoperfusion in the LAD coronary artery territory (arrow). **(b)** Resting phase short-axis perfusion MR image shows corresponding persistent hypoperfusion (arrow) at rest. **(c)** Corresponding IR image shows matching segmental DE and myocardial thinning of the antroseptal wall (arrow), consistent with an old infarct in the LAD coronary artery territory.

status. However, it remained largely restricted to research applications due to the time-consuming operator interaction required for analysis of large amounts of acquired datasets. The advent of semiautomatic and fully automatic image processing methods has helped circumvent many of these limitations, paving the way for future clinical application on a wider scale.

1. Absolute quantitative analysis: In absolute quantitative analysis, the process mainly relies on the rate of contrast agent arrival in the myocardial tissue and the induced signal enhancement. Myocardial blood flow is calculated as the arterial input rate measured in milliliters per minute (mL/min) per gram of tissue (35). The regions of interest (ROIs) for the analysis are manually defined based on myocardial sectors (American Heart Association 17-segment model) (36) or on myocardial pixels to generate perfusion maps with spatial resolution equivalent to the underlying acquired image resolution. By contouring the endocardial and epicardial borders of the LV myocardium and carefully avoiding inclusion of adjacent tissue or blood, an ROI is created through which the time-intensity curve (TIC) of contrast agent wash-in and washout can be obtained (3).

There are two major approaches used for absolute quantification of myocardial blood flow: model-independent and model-based. Model-independent approaches are based on the central volume principle introduced by Zierler (37), which starts with the observation that the rate at which a substance accumulates in an ROI in tissue represents the product of the difference of concentrations of the tracer substance flowing into and out of the region according to the flow rate. In model-based approaches, on the other hand, myocardial functional spaces are identified as well as the contrast agent flow pattern as it traverses through these spaces and as it crosses the permeable barriers in between. Since commonly used contrast agents are extracellular agents like gadopentetate dimeglumine (Gd-DTPA), the commonly applied model is a two-compartment model comprising the vascular and interstitial spaces. A detailed description of the different available analysis techniques and their underlying principles is presented in references 35 and 38.

Most quantitative analysis methods require that the measured blood enhancement data (AIF) and tissue enhancement data (tissue function [TF]) be calculated and mathematically deconvoluted to generate absolute myocardial perfusion parameters. This helps circumvent limitations posed by differences in the pharmacodynamics

and pharmacokinetic properties of the contrast agent on semiquantitatively generated upslope measures (39).

2. Semiquantitative analysis: On the other hand, semiquantitative analysis examines the mean signal intensity within an ROI over time, generating a TIC (Fig 6). A TIC represents the sampled myocardial intensity for all the time points within an ROI. Parameters derived from the TIC include peak signal intensity, upslope, time to peak, mean transit time, area under the TIC, and MPR index (38,40,41):

Peak signal intensity ( $SI_{\text{peak}}$ ) is the peak signal value of the TIC attained during the first pass of the contrast agent, relative to the baseline before contrast enhancement.

The upslope is the first derivative of the initial ascent of the first pass along the TIC and is usually normalized by the upslope of the LV blood pool.

Time to peak ( $T_{\text{peak}}$ ) is the time from onset of contrast enhancement to the peak of the TIC.

Mean transit time ( $T_{\text{mean}}$ ) is the average time required for the contrast agent to pass through the ROI.

Area under the TIC (ATIC) is the area under the TIC from the beginning of its ascent to a user-defined point.

MPR index (MPRI) is the ratio of the stress and rest perfusion upslopes, corrected for the AIF by simple division by the upslope of the curve of the ventricular cavity (40).

Among these, the upslope and MPRI have been considered the most relevant semiquantitative parameters for detection of a perfusion abnormality.

### Artifacts

Technical artifacts could hamper interpretation and analysis of cardiac MR perfusion images. Of these, dark rim artifact (DRA), occurring at the subendocardial border and occasionally confused with genuine perfusion deficits, seems to be the most common (Fig 7). Several factors have been proposed to explain it, including limited spatial resolution (42), cardiac motion (43), partial volume effects when blood and myocardium are out of phase (14), and susceptibility (44). Viewing the images in cine mode can help identify the artifact on the basis of its transient behavior (lasting only a few heartbeats compared with real hypoperfusion defects) and temporal variation as the contrast agent bolus passes through the LV blood pool.

Dark rim artifacts generally become more obvious with a higher concentration of the contrast agent bolus and are perpendicular to the phase-encoding direction. Hence, increasing the spatial resolution in the phase-encoding direction (ie,

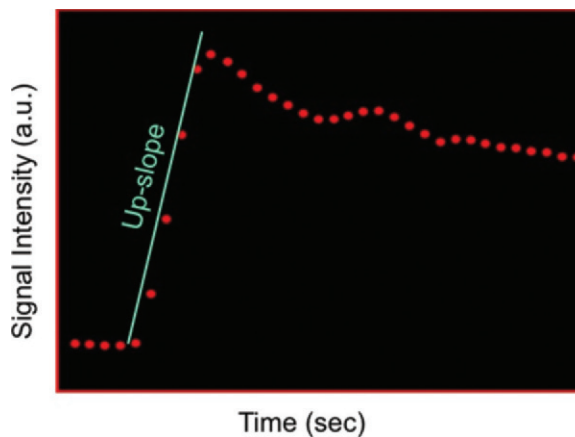


**Figure 6.** Example of a myocardial perfusion TIC generated for quantitative analysis. *a.u.* = arbitrary units.

increasing the number of phase-encoding steps) is one of the approaches suggested to minimize their occurrence. In their study incorporating DE images for improved detection of CAD, Klem et al (34) identified these artifacts as almost matched defects on the rest and stress phase images without corresponding DE defect. This underscores the role of a comprehensive viability cardiac MR study to achieve high diagnostic accuracy.

In addition to dark rim artifact, other types of artifacts may occur that affect semiquantitative and quantitative perfusion analysis. Suboptimal saturation caused by  $B_0$  and  $B_1$  field inhomogeneity can result in magnetization residue that alters the regional T1 relaxation time, ultimately leading to quantification errors in these regions. This could be overcome by using adiabatic composite (BIR-4) saturation pulses, which achieve complete saturation (45). Dark banding or susceptibility artifacts can arise in techniques that use SSFP readouts due to  $B_0$  field inhomogeneity caused by inadequate shim or susceptibility gradient associated with contrast agent bolus injection. These can be reduced by shim and center frequency readjustment (14).

On the other hand, chemical shift artifacts can interfere with GRE-EPI sequences and can be avoided by incorporation of fat-suppression pulses and phase-correction reference images. Another commonly encountered artifact is wrap or aliasing artifact, where one part of the imaged anatomy might be encoded in the same position as another. This can be corrected by in-plane rotation of the phase- and frequency-encoding directions or by increasing the phase-encoding field of view (18). Many of these artifacts can result in nondiagnostic studies if encountered after administration of the contrast agent bolus.

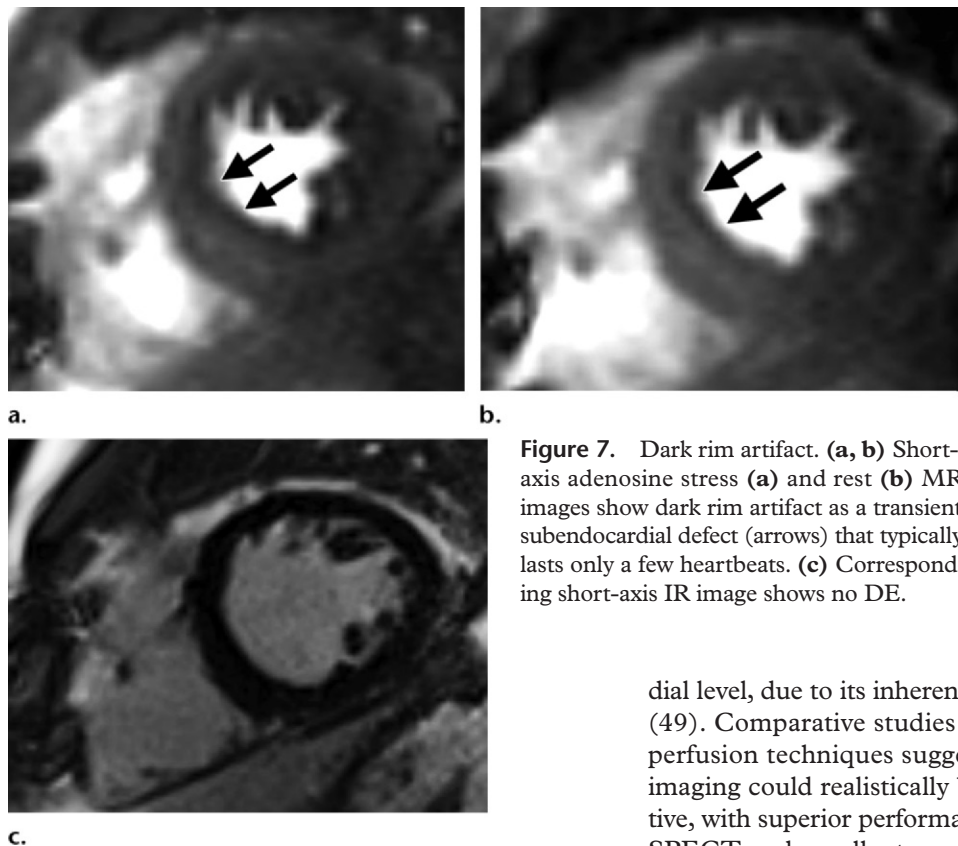


**Figure 7.** Dark rim artifact. (a, b) Short-axis adenosine stress (a) and rest (b) MR images show dark rim artifact as a transient subendocardial defect (arrows) that typically lasts only a few heartbeats. (c) Corresponding short-axis IR image shows no DE.

### Clinical Applications of Cardiac MR Perfusion Imaging

Cardiac MR perfusion imaging has demonstrated a growing role in defining the cause of chest pain, not only in the setting of flow-limiting epicardial coronary disease but also extending to the setting of underlying microangiopathy.

#### Performance of Cardiac MR Perfusion Imaging in Large-Vessel CAD

According to the American College of Cardiology expert consensus document on cardiac MR imaging issued in 2010 (46), cardiac MR stress tests combined with functional and DE imaging can serve as a primary form of CAD testing for (a) identifying patients with ischemic heart disease presenting with resting electrocardiographic abnormalities or inability to exercise, (b) identifying patients with large-vessel CAD who are candidates for interventional procedures and defining its distribution, and (c) identifying appropriate candidates for interventional procedures in the setting of CAD who will develop improvement in LV systolic function after coronary arterial revascularization.

In the setting of suspected CAD, cardiac MR imaging–quantified MPR yields high diagnostic accuracy for detection of flow-limiting coronary lesions (40,47,48), especially at the subendocar-

dial level, due to its inherent high spatial resolution (49). Comparative studies with existing nuclear perfusion techniques suggest MR perfusion imaging could realistically be used as an alternative, with superior performance relative to that of SPECT and excellent agreement with positron emission tomography (PET) perfusion data.

In their large population-based prospective trial (Clinical Evaluation of Magnetic Resonance Imaging in Coronary Heart Disease [CE-MARC]) comparing the diagnostic performance of multiparametric cardiac MR imaging and SPECT against that of coronary angiography (the standard), Greenwood et al (50) demonstrated significantly higher sensitivity and negative predictive value for cardiac MR perfusion imaging compared with SPECT: 86.5% (95% confidence interval [CI], 81.8%–90.1%) versus 66.5% (95% CI, 60.4%–72.1%) and 90.5% (95% CI, 87.1%–93.0%) versus 79.1% (95% CI, 74.8%–82.8%), respectively.

Similarly, a good correlation has been steadily confirmed for relative and absolute quantitative methods of cardiac MR perfusion imaging, with PET quantification techniques considered the reference standard (39,51). On the other hand, stress cardiac MR imaging offers the benefit of integrating cardiac MR perfusion imaging with a comprehensive assessment of global and regional function, tissue edema, and scar burden in the setting of myocardial infarction, all achieved at high spatial resolution and high tissue contrast.

Compared with invasive physiologic measurements like pressure wire–derived fractional flow reserve (FFR), cardiac MR perfusion imaging has demonstrated high diagnostic accuracy for detection of functionally significant CAD, with

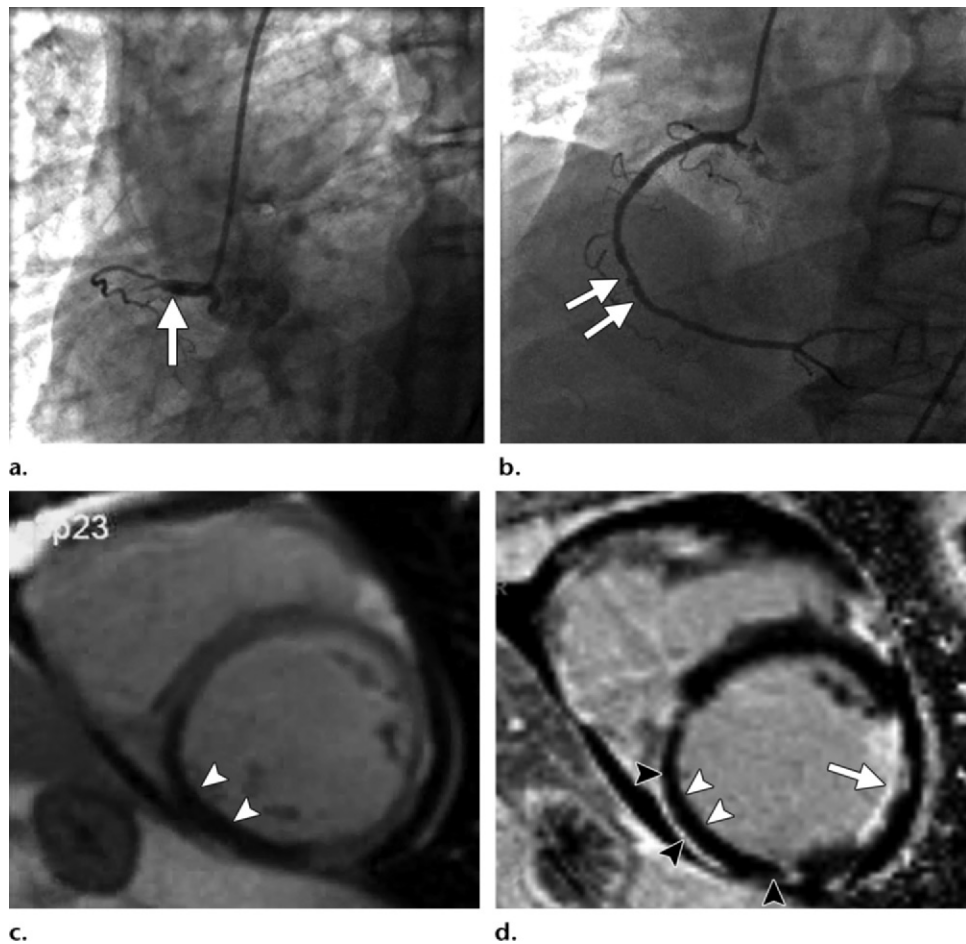


**Figure 8.** Acute transmural infarct in a 60-year-old man with acute retrosternal pain and elevated cardiac enzyme levels. **(a)** Coronary angiogram shows occlusion of the right coronary artery (RCA) (arrow). **(b)** Coronary angiogram shows successful recanalization of the RCA achieved with stent placement (arrows). **(c)** Resting short-axis perfusion MR image acquired after successful reperfusion shows persistent segmental subendocardial hypoperfusion at the infarct core in the inferior wall (arrowheads). **(d)** Corresponding short-axis DE image shows an acute transmural infarct in the RCA territory with a persistent nonenhancing core (white arrowheads), consistent with MO, surrounded by peripheral DE (black arrowheads). Also note the old myocardial infarction with wall thinning in the lateral LV wall in the territory of the left circumflex coronary artery (arrow).

91% sensitivity, 94% specificity, and positive and negative predictive values of 91% and 94%, respectively (52). With the current increased focus on physiologic data to aid appropriate lesion selection for percutaneous intervention, and evidence that FFR calculation may improve the selection process (53), noninvasive preprocedure assessment of perfusion with cardiac MR imaging is similarly likely to prove beneficial.

Two recent meta-analyses by Nandalur et al (54) and Hamon et al (55) confirmed a high sensitivity of 91% and specificity of 80%–81% for diagnosis of CAD on a per-patient basis for cardiac MR perfusion stress testing.

In patients with acute myocardial infarction, coronary reperfusion is frequently associated with microvascular obstruction (MO), seen

angiographically as “no reflow” or “low flow.” This results from prolonged ischemia causing myocardial necrosis and MO propagated by an inflammatory process, resulting in accumulation of neutrophil plugs, endothelial swelling, and compression of capillaries between swollen myocytes. After an acute myocardial infarction, the myocardium will display one of several patterns of contrast enhancement, depending on the degree of tissue perfusion with gadolinium contrast material and available extracellular space.

In the normal myocardium, T1-weighted signal intensity rapidly increases, comes to a plateau, and then decreases as the gadolinium contrast material washes out. Alternatively, the myocardial segments supplied by the infarct-related artery demonstrate two different pat-

**Table 3: Pathophysiologic Mechanisms Resulting in Microvascular Dysfunction**

<b>Structural</b>
Luminal obstruction (microemboli after myocardial infarction)
Vascular wall infiltration (amyloidosis)
Vascular remodeling (HCM, arterial hypertension)
<b>Functional</b>
Endothelial dysfunction (diabetes, smoking)
Smooth muscle cell dysfunction (HCM, arterial hypertension)
<b>Extravascular</b>
Extramural compression (HCM, aortic stenosis, arterial hypertension)

Source.—Reference 1.

Note.—HCM = hypertrophic cardiomyopathy.

terns of contrast enhancement: Peripherally, T1-weighted signal intensity increases more slowly than in normal myocardium, reaching a hyperintense plateau that persists over a period of 10 minutes. On the other hand, the infarct core remains persistently hypointense in comparison with the periphery for several minutes, denoting MO (Fig 8) (56).

**The presence of MO within the infarct bed is a marker of nonviable tissue in which function rarely recovers. In addition, MO has been associated with adverse prognosis and adverse LV remodeling independently of infarct size (57).** Several studies have demonstrated increased sensitivity of first-pass resting perfusion imaging in delineating MO (58), hence assisting in distinction of chronic from acute infarcts and serving as a prognostic marker for patient outcome in the setting of acute myocardial injury (57).

Cardiac MR perfusion imaging has also been used to assess functional recovery after percutaneous coronary interventions. Significantly improved MPR index was noted after intervention, especially after stent placement (59). Ongoing studies have uncovered a powerful role for cardiac MR perfusion imaging as a prognostic tool providing answers regarding major cardiac events in various CAD clinical scenarios. In 513 patients with known or suspected CAD, Jahnke et al (60) demonstrated 3-year event-free survival of 99.2% for patients without hypoperfusion compared to 83.5% in patients with hypoperfusion.

In addition, an incremental benefit could be added by complementing cardiac MR perfusion imaging with DE imaging in the same diagnostic setting, since scar burden has been established as another independent factor for major events

in this population (61,62). Hence, in light of the convincing evidence supporting the diagnostic and prognostic roles of cardiac MR perfusion imaging, further integration into the existing diagnostic strategies is expected in the appropriate clinical setting.

### Performance of Cardiac MR Perfusion Imaging in Small-Vessel Diseases

Primary coronary microcirculatory dysfunction (ie, small-vessel disease) in the absence of flow-limiting CAD has been shown to play a fundamental role in the pathophysiology of several cardiac pathologic conditions. The mechanism is suggested to encompass approximately 10%–30% of patients undergoing coronary angiography because of angina, who have “normal” or “near-normal” epicardial coronary arteries at angiography (63). Table 3 demonstrates the suggested underlying pathophysiologic mechanisms for small-vessel diseases.

In a study including 317 patients who were referred for suspected myocardial ischemia, Bernhardt et al (64) demonstrated that patients with hypertension and/or diabetes in whom relevant CAD was excluded at cardiac catheterization ( $n = 64$  [22%]) have a significantly higher prevalence of subendocardial ischemia at stress cardiac MR imaging compared with other patients. These findings support prior proposed mechanisms suggesting microvascular disease secondary to endothelial dysfunction as a plausible cause of angina in hypertensive and diabetic patients in the absence of CAD (56,65). The authors typically described adenosine stress-induced perfusion deficits affecting one-third or less of wall thickness with persistence for five or fewer heartbeats in this patient population (Fig 9).

In concordance with these findings, increased coronary risk factor burden (eg, diabetes and hypertension) associated with reduced mean blood flow and perfusion reserve reflecting reduced coronary vasoreactivity to adenosine stress was reported in a subset of 222 MESA (Multi-Ethnic Study of Atherosclerosis) participants free of the clinical diagnosis of heart disease. This was in turn strongly inversely correlated with estimated 10-year coronary heart disease risk based on Framingham equations ( $P$  for trends  $< .0001$ ) (66).

Multiple clinical studies have also suggested improvement of CFR with lifestyle modifications or pharmacologic intervention in this patient population (67). These findings point out the role of cardiac MR perfusion imaging as a noninvasive tool in detection of subclinical coronary disease, which may benefit patient treatment and clinical course modification.

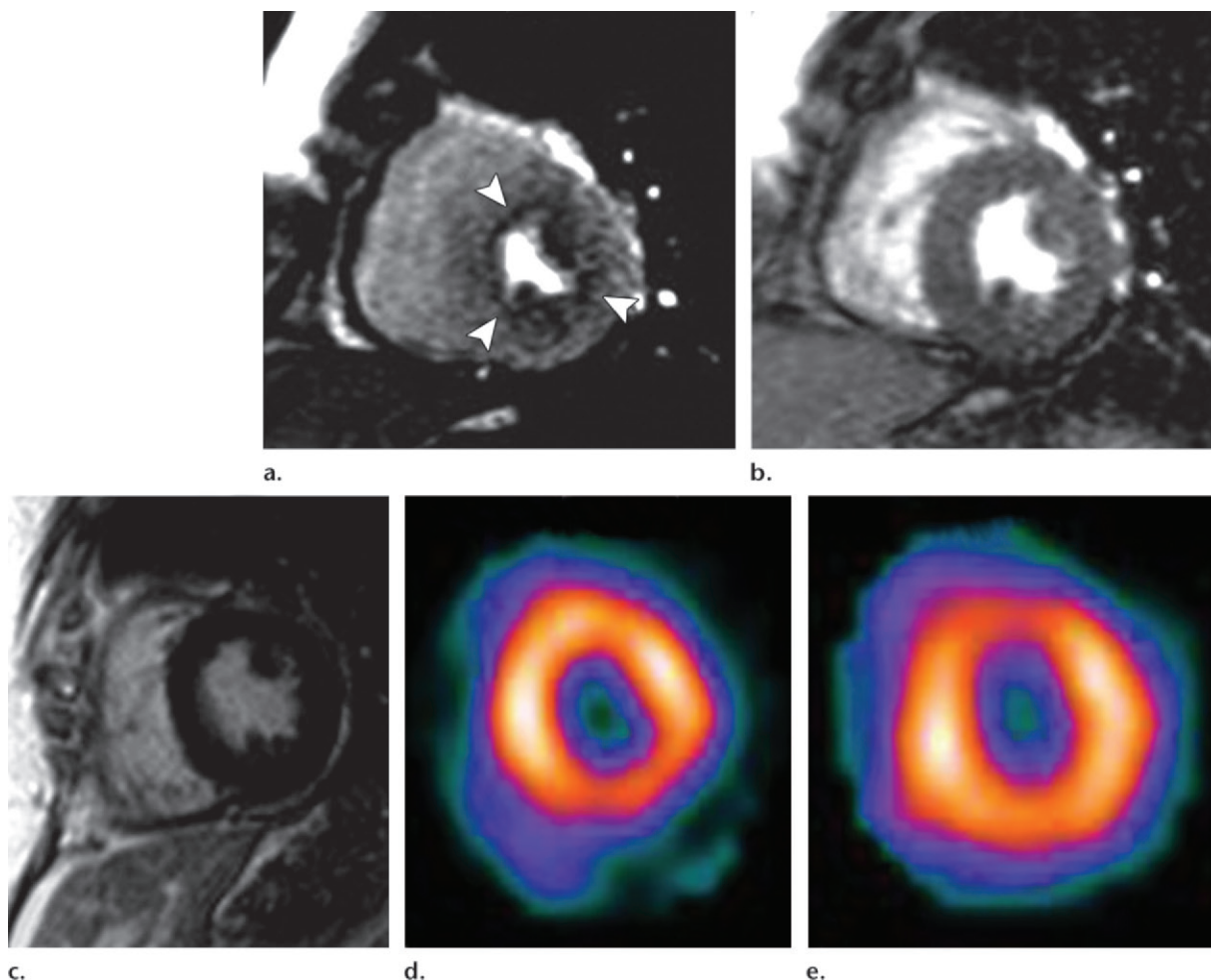


**Figure 9.** Small-vessel disease in a 53-year-old patient with a clinical history of diabetes mellitus and hypertension who presented with recurrent chest pain and negative cardiac enzyme levels. **(a)** Short-axis first-pass adenosine perfusion MR image shows diffuse subendocardial hypoperfusion (arrowheads). **(b)** Corresponding short-axis rest MR image shows no myocardial hypoperfusion. **(c)** Corresponding DE image shows no scar. **(d, e)** Corresponding stress **(d)** and rest **(e)** SPECT images show no hypoperfusion. (Reprinted, with permission, from reference 56.)

*Cardiac syndrome X* and *microvascular angina* are two terms given to a category of small-vessel disease patients who present with a certain constellation of clinical and diagnostic features (63): *(a)* effort-induced angina in the presence of normal coronary arteries at angiography with no spontaneous or inducible epicardial coronary artery spasm at ergonovine or acetylcholine provocation, such as that seen with variant angina; *(b)* ST-segment depression suggestive of myocardial ischemia during spontaneous or provoked angina; and *(c)* absence of intrinsic cardiac diseases (eg, HCM, amyloidosis) or systemic diseases (eg, hypertension, diabetes) potentially associated with microvascular dysfunction.

Diagnosed patients are described as younger and more commonly female compared to those with atherosclerotic CAD. The exact pathogenesis remains uncertain, with two mechanisms proposed involving coronary microvascular

dysfunction (ie, abnormal dilatory response and/or increased vasoconstriction) and enhanced sensitivity to intracardiac pain (the so-called “sensitive heart” syndrome) (63).

Using perfusion cardiac MR imaging, Panting et al (68) showed that MPR index was significantly reduced in the subendocardium but not in the subepicardium of such patients. Further work by Wöhrle et al (69) showed blunting of the MPR index in response to both intravenous adenosine and intracoronary acetylcholine as well as strong correlation with invasive Doppler measurements of coronary blood flow reserve.

In the latter study, cardiac syndrome X patients with an abnormal perfusion reserve were more likely to have elevated serum levels of inflammatory markers, which may suggest a potential inflammatory pathophysiologic role as cause for the microvascular dysfunction that is the hallmark of this disease. On the basis of this evidence, cardiac MR stress perfusion imaging

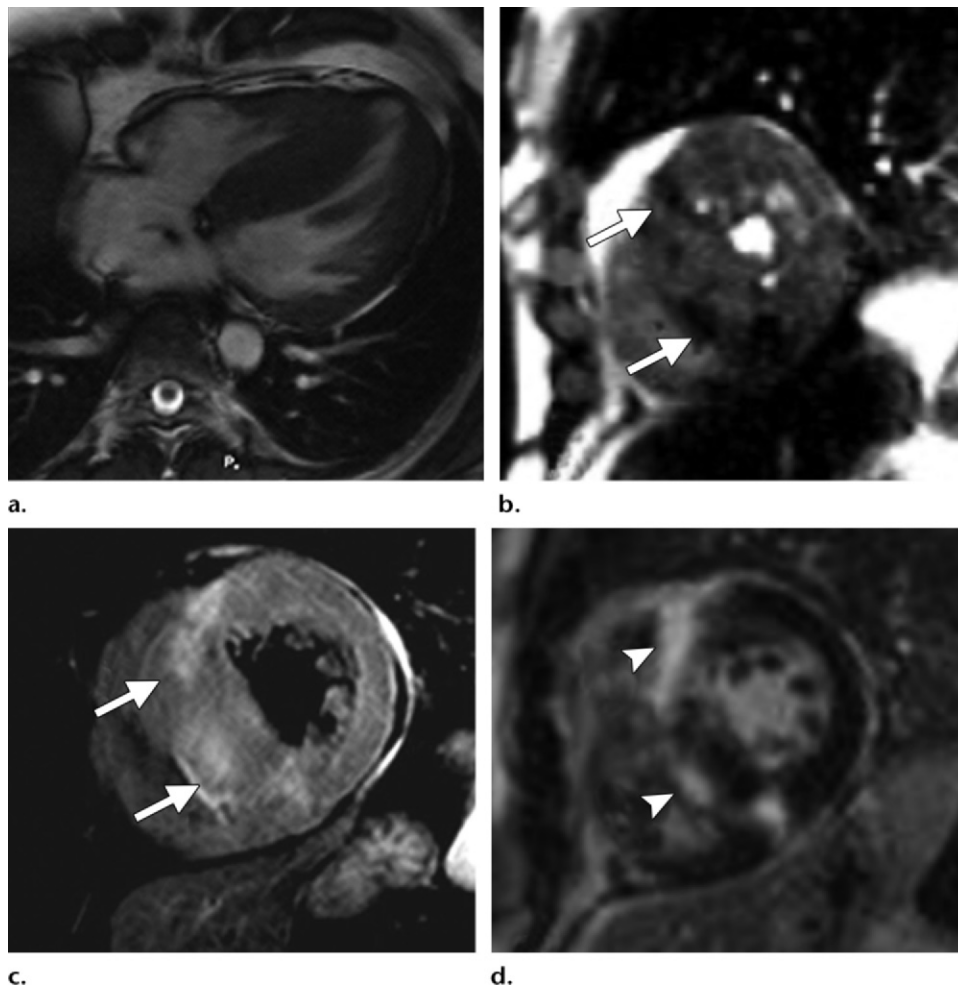


**Figure 10.** HCM in a 40-year-old man. **(a)** Four-chamber cine MR image shows septal hypertrophy. **(b)** Short-axis resting perfusion MR image shows areas of reduced myocardial perfusion (arrows) in the thickened interventricular septum. **(c)** T2-weighted MR image shows areas of increased T2 signal corresponding to the areas of hypoperfusion (arrows). **(d)** DE image shows corresponding enhancement (arrowheads).

could potentially play a promising noninvasive role in the diagnostic workup of patients with microvascular dysfunction.

### Novel Applications of Perfusion Cardiac MR Imaging in Nonischemic Cardiomyopathies and Pulmonary Hypertension

Currently, the role of cardiac MR perfusion imaging has extended beyond traditional detection of coronary epicardial diseases to unveil the potential role of microvascular dysfunction in nonischemic and infiltrative cardiomyopathies.

**Hypertrophic Cardiomyopathy.**—HCM is the most frequently occurring genetic cardiomyopathy responsible for sudden cardiac death in young trained athletes. It has an autosomal dominant pattern of inheritance, hence warranting familial screening. Underlying histopathologic changes

identified include myofibrillar disarray and abnormal intramural coronary vasculature (70).

Reduced resting myocardial perfusion (71) and reduced MPR, particularly in the endocardium, were demonstrated in HCM patients at cardiac MR perfusion imaging. These findings were associated with the degree of wall thickness and extent of scarring at DE imaging (72) (Fig 10). These results suggest that microvascular abnormalities may precede and predispose to the development of myocardial fibrosis, hence constituting important components of the risk attributable to HCM as a cause of sudden cardiac death.

**Idiopathic Dilated Cardiomyopathy.**—Idiopathic dilated cardiomyopathy (IDC) is characterized by LV or biventricular enlargement and impaired contractility of unknown cause. An autosomal dominant inherited form of the disease accounts for approximately 20%–50% of IDC cases and

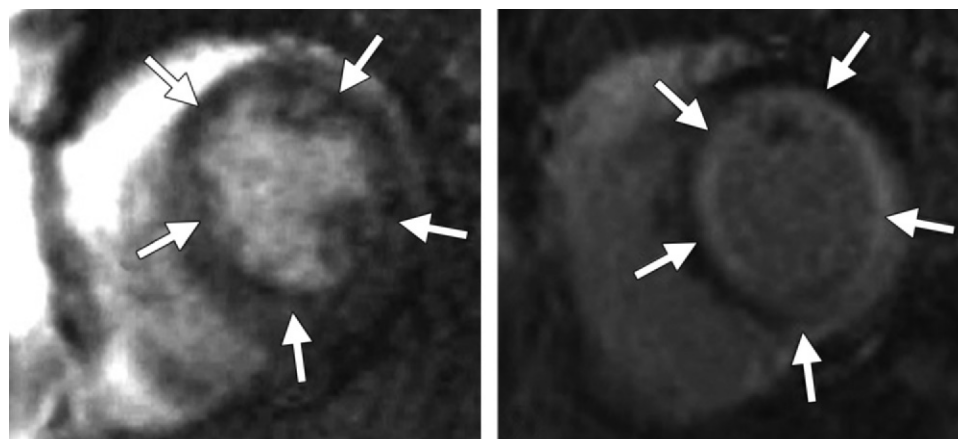


**Figure 11.** Cardiac amyloidosis diagnosed with endomyocardial biopsy in a 65-year-old man. **(a)** Short-axis resting first-pass perfusion MR image shows diffuse subendocardial hypoperfusion (arrows). **(b)** Corresponding short-axis DE image shows diffuse subendocardial contrast enhancement of the LV (arrows) sparing the midwall and epicardium. There was some difficulty nulling the myocardium due to rapid washout of gadolinium contrast material.

is termed *familial dilated cardiomyopathy*. Jerosch-Herold et al (73) reported abnormal resting blood flow in patients with IDC who were found to have increased extracellular matrix remodeling.

**Amyloidosis.**—Amyloidosis is a heterogeneous group of diseases with a common feature of extracellular deposition and infiltration of different types of amyloid fibrils in various organs including the heart. Amyloidosis patients may occasionally present clinically with symptoms similar to angina pectoris. This is thought to be secondary to intramural coronary artery amyloid deposits that reduce luminal diameter (74).

Several studies have identified different patterns of late enhancement with gadolinium contrast material; the most common is a diffuse subendocardial pattern, which has demonstrated high diagnostic accuracy for detecting cardiac amyloid when compared with endomyocardial biopsy (75). Fast washout kinetics for gadolinium contrast material resulting in suboptimal myocardial nulling on T1-weighted inversion time scout images have also been described (76). Despite that, there are few case reports that describe diffuse stress-induced subendocardial hypoperfusion denoting myocardial ischemia (77). In our clinical experience, subendocardial hypoperfusion is also noted at rest, corresponding to areas of DE (Fig 11).

**Cardiac Sarcoidosis.**—Sarcoidosis is a systemic inflammatory disease pathologically characterized by noncaseating granulomas. Although cardiac involvement is clinically evident in only 5% of patients, autopsy studies show myocardial involvement in up to 50% of cases of fatal sarcoidosis. Cardiac involve-

ment may cause congestive heart failure, supraventricular and ventricular arrhythmias, conduction disturbances, and sudden cardiac death.

Compared with other imaging modalities, cardiac MR has demonstrated high sensitivity and specificity in early diagnosis of sarcoidosis. Focal hyperintensity on T2-weighted images in the active phase of the disease as well as several DE patterns predominantly involving the base and lateral wall of the LV have been described, correlating with the clinical course of the disease (78). In a recent pilot study, Mavrogeni et al (79) reported reduced MPR and diffuse fibrosis in the absence of DE in asymptomatic patients. These findings suggest that microvascular dysfunction may constitute an early component of the disease preceding granuloma formation and contributing to LV dysfunction (Fig 12).

**Pulmonary Arterial Hypertension.**—Biventricular vasoreactivity measured with adenosine stress cardiac MR imaging is significantly reduced in pulmonary arterial hypertension (PAH) and inversely correlated with right ventricular (RV) workload and ejection fraction, suggesting that reduced MPR may contribute to RV dysfunction in patients with PAH (Fig 13) (80).

There are several mechanisms whereby PAH may lead to reduced RV MPR and thus to myocardial ischemia: Marked RV remodeling with RV myocardial hypertrophy results in increased wall tension, which leads to decreased oxygen supply, increased oxygen extraction, and decreased perfusion secondary to compression of the coronary circulation. Furthermore, systemic hypotension, common in PAH and partially related to ventric-

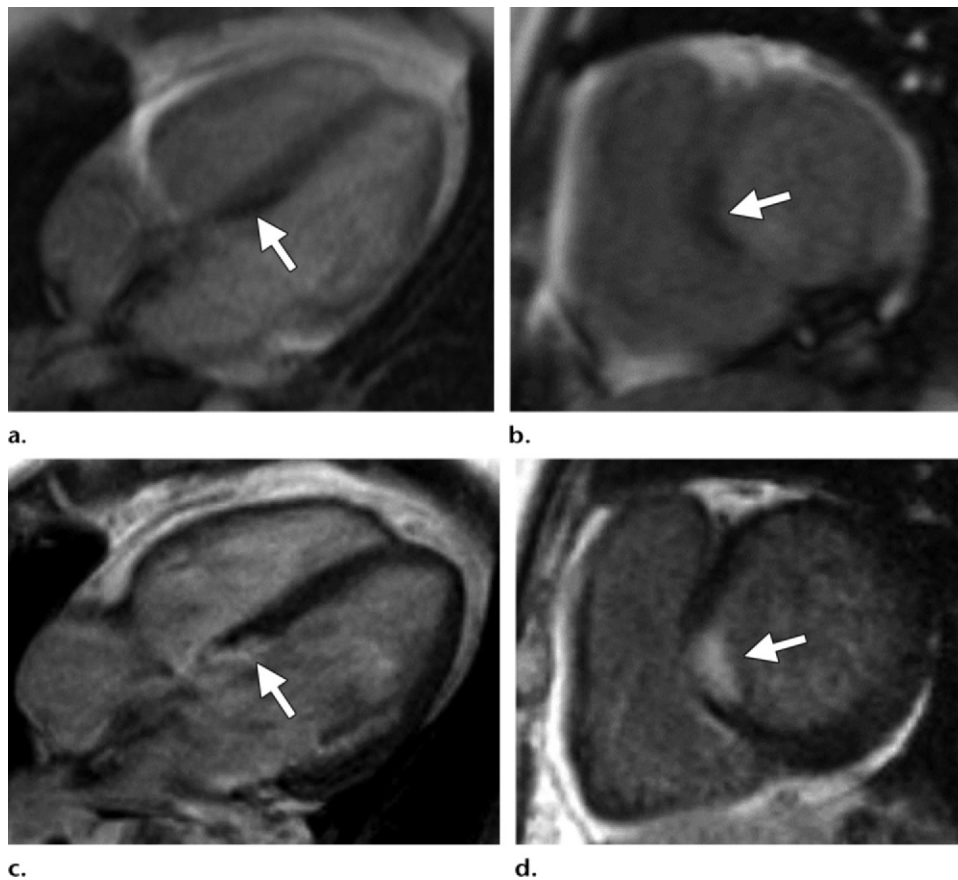


**Figure 12.** Newly diagnosed sarcoidosis in a 37-year-old woman with intermittent third-degree heart block. (**a, b**) Four-chamber (**a**) and short-axis (**b**) resting perfusion MR images show a focal area of hypoperfusion at the basal interventricular septum (arrow). (**c, d**) Corresponding four-chamber (**c**) and short-axis (**d**) IR MR images show matching focal delayed hyperenhancement (arrow).

ular interdependence, leads to decreased coronary driving pressure, especially when pulmonary artery pressures are equal to or higher than systemic pressures. Aside from these hemodynamic alterations, a dysfunctional microcirculation such as that seen in scleroderma or idiopathic PAH may further contribute to decreased vasoreactivity and tissue ischemia (81).

### Limitations

Several limitations still exist hampering wide clinical implementation of cardiac MR perfusion imaging. Gadolinium-based agents are still used off-label for cardiac perfusion imaging due to lack of regulatory approval. In addition, administration of vasodilator stress agents (eg, adenosine) in the MR imaging environment is still considered more challenging compared with other modalities (eg, PET or SPECT), requiring additional safety precautions. This limitation may be partly overcome with use of regadenoson, newly approved by the U.S. Food and Drug Administration, which offers easier administration, comparable efficacy, and reduced side effects compared with the widely used stress agents.

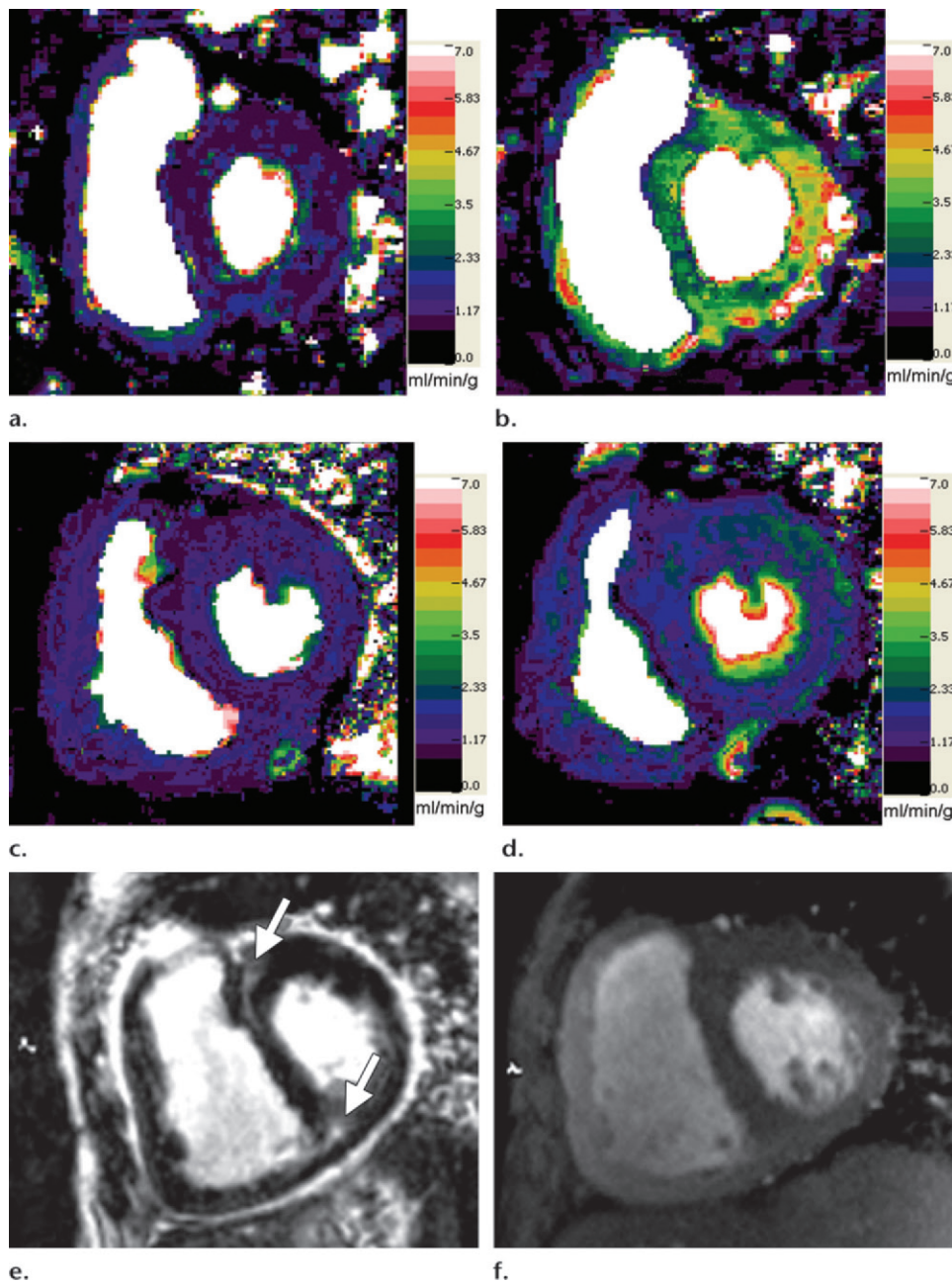
Lack of complete cardiac coverage is another technical limitation of cardiac MR imaging compared with other perfusion imaging modalities including SPECT. According to recently published data, highly accelerated three-dimensional image acquisition with high-field-strength (3-T) magnets holds great prospects for covering the whole ventricle in one heartbeat with acceptable spatial resolution, hence improving the diagnostic performance of cardiac MR imaging (20,82).

Finally, to overcome the limitations of imaging patients with pacemakers and implantable cardiac defibrillators, cardiac device manufacturers are currently providing MR imaging-compatible or -conditional pacemaker devices. Efforts are under way to provide similar implantable cardiac defibrillators.

### Conclusion

Cardiac MR perfusion imaging has evolved to become a powerful clinical tool for diagnosis and management of many cardiac conditions. In addition to its role in improving detection of clinically

**Figure 13.** (a, b) Short-axis perfusion maps of the RV and LV at rest (a) and during adenosine-induced stress (b) in a healthy control subject. A perfusion scale is shown at right. (c, d) Short-axis perfusion maps of the RV and LV at rest (c) and during stress (d) in a PAH patient (mean pulmonary artery pressure, 45 mm Hg). Lower RV and LV MPR indexes are seen in the PAH patient (blue and purple color coding) than in the control subject. (e) Short-axis DE image shows scarring (arrows) at the RV septal insertion, a pattern described in PAH patients. (f) Short-axis cine image shows RV hypertrophy and septal flattening.



relevant CAD, it has also offered further insights into the understanding of various cardiovascular disorders resulting from coronary microvascular dysfunction in the absence of proximal flow-limiting CAD. Recent growing clinical and prognostic data support its incorporation as a standard part of a comprehensive cardiac MR imaging examination to provide an accurate assessment of myocardial structure and function.

## References

1. Camici PG, Crea F. Coronary microvascular dysfunction. *N Engl J Med* 2007;356(8):830–840.
2. Gould KL, Lipscomb K. Effects of coronary stenoses on coronary flow reserve and resistance. *Am J Cardiol* 1974;34(1):48–55.
3. Coelho-Filho OR, Rickers C, Kwong RY, Jersch-Herold M. MR myocardial perfusion imaging. *Radiology* 2013;266(3):701–715.
4. Miller DD, Holmvang G, Gill JB, et al. MRI detection of myocardial perfusion changes by gadolinium-DTPA infusion during dipyridamole hyperemia. *Magn Reson Med* 1989;10(2):246–255.
5. Atkinson DJ, Burstein D, Edelman RR. First-pass cardiac perfusion: evaluation with ultrafast MR imaging. *Radiology* 1990;174(3 Pt 1):757–762.
6. Gerber BL, Bluemke DA, Chin BB, et al. Single-vessel coronary artery stenosis: myocardial perfusion imaging with Gadomer-17 first-pass MR imaging in a swine model of comparison with gadopentetate dimeglumine. *Radiology* 2002;225(1):104–112.
7. Niedermayer S, Prompona M, Cyran CC, Reiser M, Huber A. Dose response of the intravascular contrast agent gadofosveset trisodium in MR perfusion imaging.

- ing of the myocardium using semiquantitative evaluation. *J Magn Reson Imaging* 2014;39(1):203–210.
8. Epstein FH, Meyer CH. Myocardial perfusion using arterial spin labeling cardiac MR: promise and challenges. *JACC Cardiovasc Imaging* 2011;4(12):1262–1264.
  9. Arnold JR, Karamitsos TD, Bhamra-Ariza P, et al. Myocardial oxygenation in coronary artery disease: insights from blood oxygen level-dependent magnetic resonance imaging at 3 tesla. *J Am Coll Cardiol* 2012;59(22):1954–1964.
  10. Raman SV, Dickerson JA, Jekic M, et al. Real-time cine and myocardial perfusion with treadmill exercise stress cardiovascular magnetic resonance in patients referred for stress SPECT. *J Cardiovasc Magn Reson* 2010;12:41.
  11. Kramer CM, Barkhausen J, Flamm SD, Kim RJ, Nagel E; Society for Cardiovascular Magnetic Resonance Board of Trustees Task Force on Standardized Protocols. Standardized cardiovascular magnetic resonance (cardiac MR) protocols 2013 update. *J Cardiovasc Magn Reson* 2013;15:91.
  12. Al Jaroudi W, Iskandrian AE. Regadenoson: a new myocardial stress agent. *J Am Coll Cardiol* 2009;54(13):1123–1130.
  13. Vasu S, Bandettini WP, Hsu LY, et al. Regadenoson and adenosine are equivalent vasodilators and are superior than dipyridamole: a study of first pass quantitative perfusion cardiovascular magnetic resonance. *J Cardiovasc Magn Reson* 2013;15:85.
  14. Kellman P, Arai AE. Imaging sequences for first pass perfusion: a review. *J Cardiovasc Magn Reson* 2007;9(3):525–537.
  15. Ding S, Wolff SD, Epstein FH. Improved coverage in dynamic contrast-enhanced cardiac MRI using interleaved gradient-echo EPI. *Magn Reson Med* 1998;39(4):514–519.
  16. Wang Y, Moin K, Akinboboye O, Reichel N. Myocardial first pass perfusion: steady-state free precession versus spoiled gradient echo and segmented echo planar imaging. *Magn Reson Med* 2005;54(5):1123–1129.
  17. Fritz-Hansen T, Rostrup E, Ring PB, Larsson HB. Quantification of gadolinium-DTPA concentrations for different inversion times using an IR-turbo flash pulse sequence: a study on optimizing multislice perfusion imaging. *Magn Reson Imaging* 1998;16(8):893–899.
  18. Gerber BL, Raman SV, Nayak K, et al. Myocardial first-pass perfusion cardiovascular magnetic resonance: history, theory, and current state of the art. *J Cardiovasc Magn Reson* 2008;10:18.
  19. Niendorf T, Sodickson DK. Parallel imaging in cardiovascular MRI: methods and applications. *NMR Biomed* 2006;19(3):325–341.
  20. Jogiya R, Kozerke S, Morton G, et al. Validation of dynamic 3-dimensional whole heart magnetic resonance myocardial perfusion imaging against fractional flow reserve for the detection of significant coronary artery disease. *J Am Coll Cardiol* 2012;60(8):756–765.
  21. Tsao J, Boesiger P, Pruessmann KP. k-t BLAST and k-t SENSE: dynamic MRI with high frame rate exploiting spatiotemporal correlations. *Magn Reson Med* 2003;50(5):1031–1042.
  22. Vitanis V, Manka R, Giese D, et al. High resolution three-dimensional cardiac perfusion imaging using compartment-based k-t principal component analysis. *Magn Reson Med* 2011;65(2):575–587.
  23. Otazo R, Kim D, Axel L, Sodickson DK. Combination of compressed sensing and parallel imaging for highly accelerated first-pass cardiac perfusion MRI. *Magn Reson Med* 2010;64(3):767–776.
  24. Gutberlet M, Noeske R, Schwinge K, Freyhardt P, Felix R, Niendorf T. Comprehensive cardiac magnetic resonance imaging at 3.0 tesla: feasibility and implications for clinical applications. *Invest Radiol* 2006;41(2):154–167.
  25. Hinton DP, Wald LL, Pitts J, Schmitt F. Comparison of cardiac MRI on 1.5 and 3.0 tesla clinical whole body systems. *Invest Radiol* 2003;38(7):436–442.
  26. Nagel E, al-Saadi N, Fleck E. Cardiovascular magnetic resonance: myocardial perfusion. *Herz* 2000;25(4):409–416.
  27. Wendland MF, Saeed M, Yu KK, et al. Inversion recovery EPI of bolus transit in rat myocardium using intravascular and extravascular gadolinium-based MR contrast media: dose effects on peak signal enhancement. *Magn Reson Med* 1994;32(3):319–329.
  28. Kellman P, Aletras AH, Hsu LY, McVeigh ER, Arai AE. T2\* measurement during first-pass contrast-enhanced cardiac perfusion imaging. *Magn Reson Med* 2006;56(5):1132–1134.
  29. Christian TF, Rettmann DW, Aletras AH, et al. Absolute myocardial perfusion in canines measured by using dual-bolus first-pass MR imaging. *Radiology* 2004;232(3):677–684.
  30. Hsu LY, Rhoads KL, Holly JE, Kellman P, Aletras AH, Arai AE. Quantitative myocardial perfusion analysis with a dual-bolus contrast-enhanced first-pass MRI technique in humans. *J Magn Reson Imaging* 2006;23(3):315–322.
  31. Elkington AG, He T, Gatehouse PD, Prasad SK, Firmin DN, Pennell DJ. Optimization of the arterial input function for myocardial perfusion cardiovascular magnetic resonance. *J Magn Reson Imaging* 2005;21(4):354–359.
  32. Gatehouse PD, Elkington AG, Ablitt NA, Yang GZ, Pennell DJ, Firmin DN. Accurate assessment of the arterial input function during high-dose myocardial perfusion cardiovascular magnetic resonance. *J Magn Reson Imaging* 2004;20(1):39–45.
  33. Kim D, Axel L. Multislice, dual-imaging sequence for increasing the dynamic range of the contrast-enhanced blood signal and CNR of myocardial enhancement at 3T. *J Magn Reson Imaging* 2006;23(1):81–86.
  34. Klem I, Heitner JF, Shah DJ, et al. Improved detection of coronary artery disease by stress perfusion cardiovascular magnetic resonance with the use of delayed enhancement infarction imaging. *J Am Coll Cardiol* 2006;47(8):1630–1638.
  35. Jerosch-Herold M. Quantification of myocardial perfusion by cardiovascular magnetic resonance. *J Cardiovasc Magn Reson* 2010;12:57.
  36. Cerqueira MD, Weissman NJ, Dilsizian V, et al. Standardized myocardial segmentation and nomenclature for tomographic imaging of the heart. A statement for healthcare professionals from the Cardiac Imaging Committee of the Council on Clinical Cardiology of the American Heart Association. *Circulation* 2002;105(4):539–542.
  37. Zierler KL. Equations for measuring blood flow by external monitoring of radioisotopes. *Circ Res* 1965;16:309–321.
  38. Jerosch-Herold M, Seethamraju RT, Swingen CM, Wilke NM, Stillman AE. Analysis of myocardial

- perfusion MRI. *J Magn Reson Imaging* 2004;19(6):758–770.
39. Bratis K, Mahmoud I, Chiribiri A, Nagel E. Quantitative myocardial perfusion imaging by cardiovascular magnetic resonance and positron emission tomography. *J Nucl Cardiol* 2013;20(5):860–870; quiz 857–859, 871–873.
  40. Al-Saadi N, Nagel E, Gross M, et al. Noninvasive detection of myocardial ischemia from perfusion reserve based on cardiovascular magnetic resonance. *Circulation* 2000;101(12):1379–1383.
  41. Keijer JT, van Rossum AC, van Eenige MJ, et al. Semiquantitation of regional myocardial blood flow in normal human subjects by first-pass magnetic resonance imaging. *Am Heart J* 1995;130(4):893–901.
  42. Di Bella EV, Parker DL, Sinusas AJ. On the dark rim artifact in dynamic contrast-enhanced MRI myocardial perfusion studies. *Magn Reson Med* 2005;54(5):1295–1299.
  43. Storey P, Chen Q, Li W, Edelman RR, Prasad PV. Band artifacts due to bulk motion. *Magn Reson Med* 2002;48(6):1028–1036.
  44. Schreiber WG, Schmitt M, Kalden P, Mohrs OK, Kreitner KF, Thelen M. Dynamic contrast-enhanced myocardial perfusion imaging using saturation-prepared TrueFISP. *J Magn Reson Imaging* 2002;16(6):641–652.
  45. Kim D, Cernicanu A, Axel L. B(0) and B(1)-insensitive uniform T(1)-weighting for quantitative, first-pass myocardial perfusion magnetic resonance imaging. *Magn Reson Med* 2005;54(6):1423–1429.
  46. American College of Cardiology Foundation Task Force on Expert Consensus Documents, Hundley WG, Bluemke DA, et al. ACCF/ACR/AHA/NASCI/SCMR 2010 expert consensus document on cardiovascular magnetic resonance: a report of the American College of Cardiology Foundation Task Force on Expert Consensus Documents. *J Am Coll Cardiol* 2010;55(23):2614–2662.
  47. Cullen JH, Horsfield MA, Reek CR, Cherryman GR, Barnett DB, Samani NJ. A myocardial perfusion reserve index in humans using first-pass contrast-enhanced magnetic resonance imaging. *J Am Coll Cardiol* 1999;33(5):1386–1394.
  48. Nagel E, Klein C, Paetsch I, et al. Magnetic resonance perfusion measurements for the noninvasive detection of coronary artery disease. *Circulation* 2003;108(4):432–437.
  49. Wagner A, Mahrholdt H, Holly TA, et al. Contrast-enhanced MRI and routine single photon emission computed tomography (SPECT) perfusion imaging for detection of subendocardial myocardial infarcts: an imaging study. *Lancet* 2003;361(9355):374–379.
  50. Greenwood JP, Maredia N, Younger JF, et al. Cardiovascular magnetic resonance and single-photon emission computed tomography for diagnosis of coronary heart disease (CE-MARC): a prospective trial. *Lancet* 2012;379(9814):453–460.
  51. Morton G, Chiribiri A, Ishida M, et al. Quantification of absolute myocardial perfusion in patients with coronary artery disease: comparison between cardiovascular magnetic resonance and positron emission tomography. *J Am Coll Cardiol* 2012;60(16):1546–1555.
  52. Watkins S, McGeoch R, Lyne J, et al. Validation of magnetic resonance myocardial perfusion imaging with fractional flow reserve for the detection of significant coronary heart disease. *Circulation* 2009;120(22):2207–2213.
  53. Tonino PA, De Bruyne B, Pijls NH, et al. Fractional flow reserve versus angiography for guiding percutaneous coronary intervention. *N Engl J Med* 2009;360(3):213–224.
  54. Nandalur KR, Dwamena BA, Choudhri AF, Nandalur MR, Carlos RC. Diagnostic performance of stress cardiac magnetic resonance imaging in the detection of coronary artery disease: a meta-analysis. *J Am Coll Cardiol* 2007;50(14):1343–1353.
  55. Hamon M, Fau G, Née G, Ehtisham J, Morello R, Hamon M. Meta-analysis of the diagnostic performance of stress perfusion cardiovascular magnetic resonance for detection of coronary artery disease. *J Cardiovasc Magn Reson* 2010;12(1):29.
  56. Vogel-Claussen J, Skrok J, Dombroski D, et al. Comprehensive adenosine stress perfusion MRI defines the etiology of chest pain in the emergency room: comparison with nuclear stress test. *J Magn Reson Imaging* 2009;30(4):753–762.
  57. Wu KC, Zerhouni EA, Judd RM, et al. Prognostic significance of microvascular obstruction by magnetic resonance imaging in patients with acute myocardial infarction. *Circulation* 1998;97(8):765–772.
  58. Mather AN, Lockie T, Nagel E, et al. Appearance of microvascular obstruction on high resolution first-pass perfusion, early and late gadolinium enhancement cardiac MR in patients with acute myocardial infarction. *J Cardiovasc Magn Reson* 2009;11:33.
  59. Al-Saadi N, Nagel E, Gross M, et al. Improvement of myocardial perfusion reserve early after coronary intervention: assessment with cardiac magnetic resonance imaging. *J Am Coll Cardiol* 2000;36(5):1557–1564.
  60. Jahnke C, Nagel E, Gebker R, et al. Prognostic value of cardiac magnetic resonance stress tests: adenosine stress perfusion and dobutamine stress wall motion imaging. *Circulation* 2007;115(13):1769–1776.
  61. Macwar RR, Williams BA, Shirani J. Prognostic value of adenosine cardiac magnetic resonance imaging in patients presenting with chest pain. *Am J Cardiol* 2013;112(1):46–50.
  62. Steel K, Broderick R, Gandla V, et al. Complementary prognostic values of stress myocardial perfusion and late gadolinium enhancement imaging by cardiac magnetic resonance in patients with known or suspected coronary artery disease. *Circulation* 2009;120(14):1390–1400.
  63. Crea F, Lanza GA. Angina pectoris and normal coronary arteries: cardiac syndrome X. *Heart* 2004;90(4):457–463.
  64. Bernhardt P, Levenson B, Albrecht A, Engels T, Strohm O. Detection of cardiac small vessel disease by adenosine-stress magnetic resonance. *Int J Cardiol* 2007;121(3):261–266.
  65. Cannon RO 3rd, Watson RM, Rosing DR, Epstein SE. Angina caused by reduced vasodilator reserve of the small coronary arteries. *J Am Coll Cardiol* 1983;1(6):1359–1373.
  66. Wang L, Jerosch-Herold M, Jacobs DR Jr, Shahar E, Folsom AR. Coronary risk factors and myocardial perfusion in asymptomatic adults: the Multi-Ethnic Study of Atherosclerosis (MESA). *J Am Coll Cardiol* 2006;47(3):565–572.
  67. Czernin J, Barnard RJ, Sun KT, et al. Effect of short-term cardiovascular conditioning and low-fat diet on myocardial blood flow and flow reserve. *Circulation* 1995;92(2):197–204.
  68. Panting JR, Gatehouse PD, Yang G-Z, et al. Abnormal subendocardial perfusion in cardiac syndrome

- X detected by cardiovascular magnetic resonance imaging. *N Engl J Med* 2002;346(25):1948–1953.
69. Wöhrle J, Nusser T, Merkle N, et al. Myocardial perfusion reserve in cardiovascular magnetic resonance: correlation to coronary microvascular dysfunction. *J Cardiovasc Magn Reson* 2006;8(6):781–787.
  70. Maron BJ. Hypertrophic cardiomyopathy: a systematic review. *JAMA* 2002;287(10):1308–1320.
  71. Hueper K, Zapf A, Skrok J, et al. In hypertrophic cardiomyopathy reduction of relative resting myocardial blood flow is related to late enhancement, T2-signal and LV wall thickness. *PLoS ONE* 2012;7(7):e41974.
  72. Petersen SE, Jerosch-Herold M, Hudsmith LE, et al. Evidence for microvascular dysfunction in hypertrophic cardiomyopathy: new insights from multiparametric magnetic resonance imaging. *Circulation* 2007;115(18):2418–2425.
  73. Jerosch-Herold M, Sheridan DC, Kushner JD, et al. Cardiac magnetic resonance imaging of myocardial contrast uptake and blood flow in patients affected with idiopathic or familial dilated cardiomyopathy. *Am J Physiol Heart Circ Physiol* 2008;295(3):H1234–H1242.
  74. Neben-Wittich MA, Wittich CM, Mueller PS, Larson DR, Gertz MA, Edwards WD. Obstructive intramural coronary amyloidosis and myocardial ischemia are common in primary amyloidosis. *Am J Med* 2005;118(11):1287.
  75. Vogelsberg H, Mahrholdt H, Deluigi CC, et al. Cardiovascular magnetic resonance in clinically suspected cardiac amyloidosis: noninvasive imaging compared to endomyocardial biopsy. *J Am Coll Cardiol* 2008;51(10):1022–1030.
  76. Maceira AM, Joshi J, Prasad SK, et al. Cardiovascular magnetic resonance in cardiac amyloidosis. *Circulation* 2005;111(2):186–193.
  77. Seeger A, Klumpp B, Kramer U, et al. MRI assessment of cardiac amyloidosis: experience of six cases with review of the current literature. *Br J Radiol* 2009;82(976):337–342.
  78. Shehata ML, Turkbey EB, Vogel-Claussen J, Bluemke DA. Role of cardiac magnetic resonance imaging in assessment of nonischemic cardiomyopathies. *Top Magn Reson Imaging* 2008;19(1):43–57.
  79. Mavrogeni S, Kouranos V, Sfrikakis PP, et al. Myocardial stress perfusion-fibrosis imaging pattern in sarcoidosis, assessed by cardiovascular magnetic resonance imaging. *Int J Cardiol* 2014;172(2):501–503.
  80. Vogel-Claussen J, Skrok J, Shehata ML, et al. Right and left ventricular myocardial perfusion reserves correlate with right ventricular function and pulmonary hemodynamics in patients with pulmonary arterial hypertension. *Radiology* 2011;258(1):119–127.
  81. Bogaard HJ, Abe K, Vonk Noordegraaf A, Voelkel NF. The right ventricle under pressure: cellular and molecular mechanisms of right-heart failure in pulmonary hypertension. *Chest* 2009;135(3):794–804.
  82. Vogel-Claussen J. Will 3D at 3-T make myocardial stress perfusion magnetic resonance imaging even more competitive? *J Am Coll Cardiol* 2012;60(8):766–767.

## MR Myocardial Perfusion Imaging: Insights on Techniques, Analysis, Interpretation, and Findings

*Monda L. Shehata, MD • Tamer A. Basha, PhD • Mohammad R. Hayeri, MD • Dagmar Hartung, MD • Oleg M. Teytelboym, MD • Jens Vogel-Claussen, MD*

**RadioGraphics 2014; 34:1636–1657 • Published online 10.1148/rg.346140074 • Content Codes:**  

### Page 1637

While myocardial blood flow may remain normal for up to ~85% luminal diameter stenosis of the epicardial artery at rest, it is reduced during maximal hyperemia when the luminal diameter falls below 50%, thus unveiling underlying autoregulatory decompensation at the level of the coronary microvascular bed.

### Page 1640

All perfusion imaging sequences entail dynamic imaging of the heart to allow a fraction-of-a-heartbeat acquisition that is repeated over a number of heartbeats to track the first pass and washout of the contrast agent bolus.

### Page 1644

Hypoperfused myocardium is generally identified as a hypointense area compared with remote (ie, normal) myocardium. A reversible stress-induced area of myocardial hypoperfusion usually lasting for eight heartbeats or longer in the absence of DE is consistent with underlying coronary ischemia. An area of irreversible myocardial hypoperfusion with matched DE is seen in the setting of myocardial infarction or scarring.

### Page 1646

Among these, the upslope and MPRI have been considered the most relevant semiquantitative parameters for detection of a perfusion abnormality.

### Page 1649

The presence of MO within the infarct bed is a marker of nonviable tissue in which function rarely recovers. In addition, MO has been associated with adverse prognosis and adverse LV remodeling independently of infarct size.